SFVTT

CFAR COLLÈGE FRANÇAIS DES ANESTHÉSISTES RÉANIMATEURS

DPC

Physiopathologie du Choc Hémorragique

PM Mertes

Service d'Anesthésie Réanimation

Nouvel Hôpital Civil – CHU de Strasbourg

U 1116 /EA 3072 /FMTS

paul-michel.mertes@chru-strasbourg.fr

Les Hôpitaux Universitaires de STRASBOURG

SFAR Société Française d'Anesthésie et de Réanimation

SFVTT

Déclaration de conflits d'intérêts

☐ **Je n'ai pas de conflit d'intérêt**

Choc Hémorragique – Situations Cliniques

- **Traumatismes graves**
- **Hémorragies obstétricales**
- **Hémorragies gastro-intestinales**
- **Chirurgie Cardio-Vasculaire (ECLS, LVAD…)**

Hémorragie: 1ère cause de décès précoce

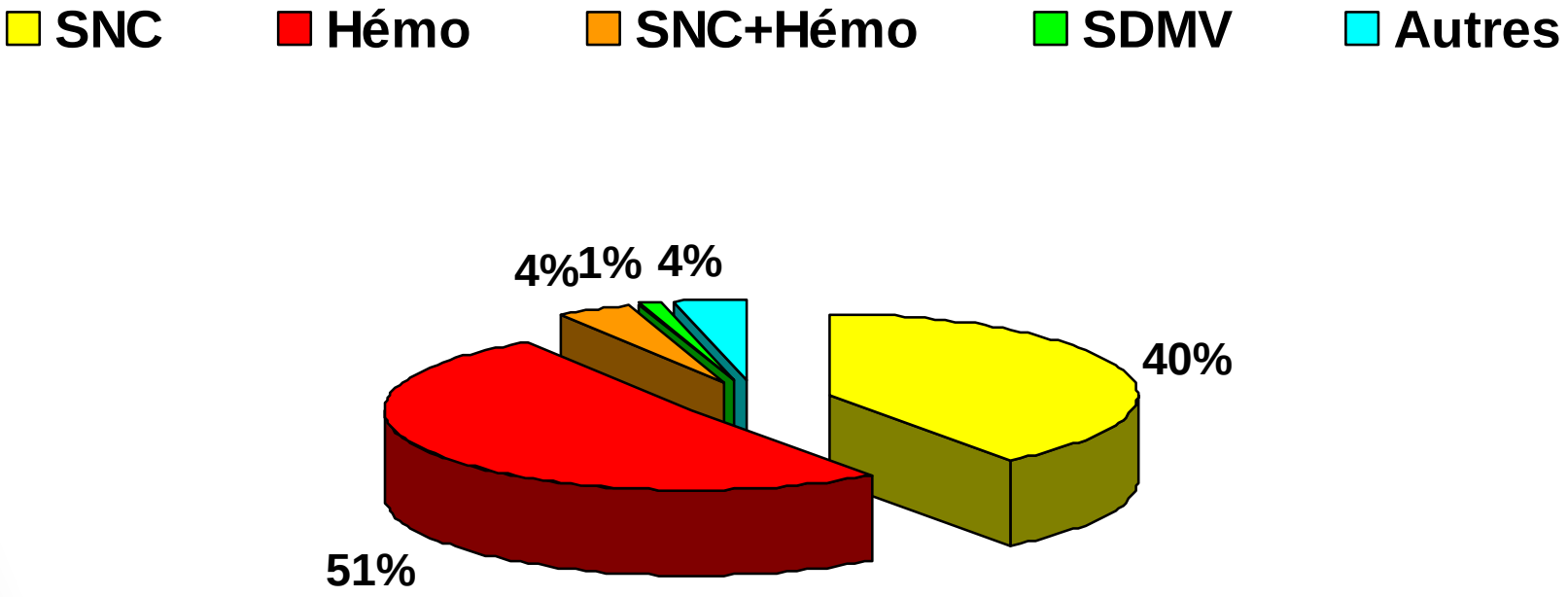

* Décès précoce < 48 h (n=154)

Sauaia et al., J Trauma 1995

Survey of Anesthesia-related Mortality in France

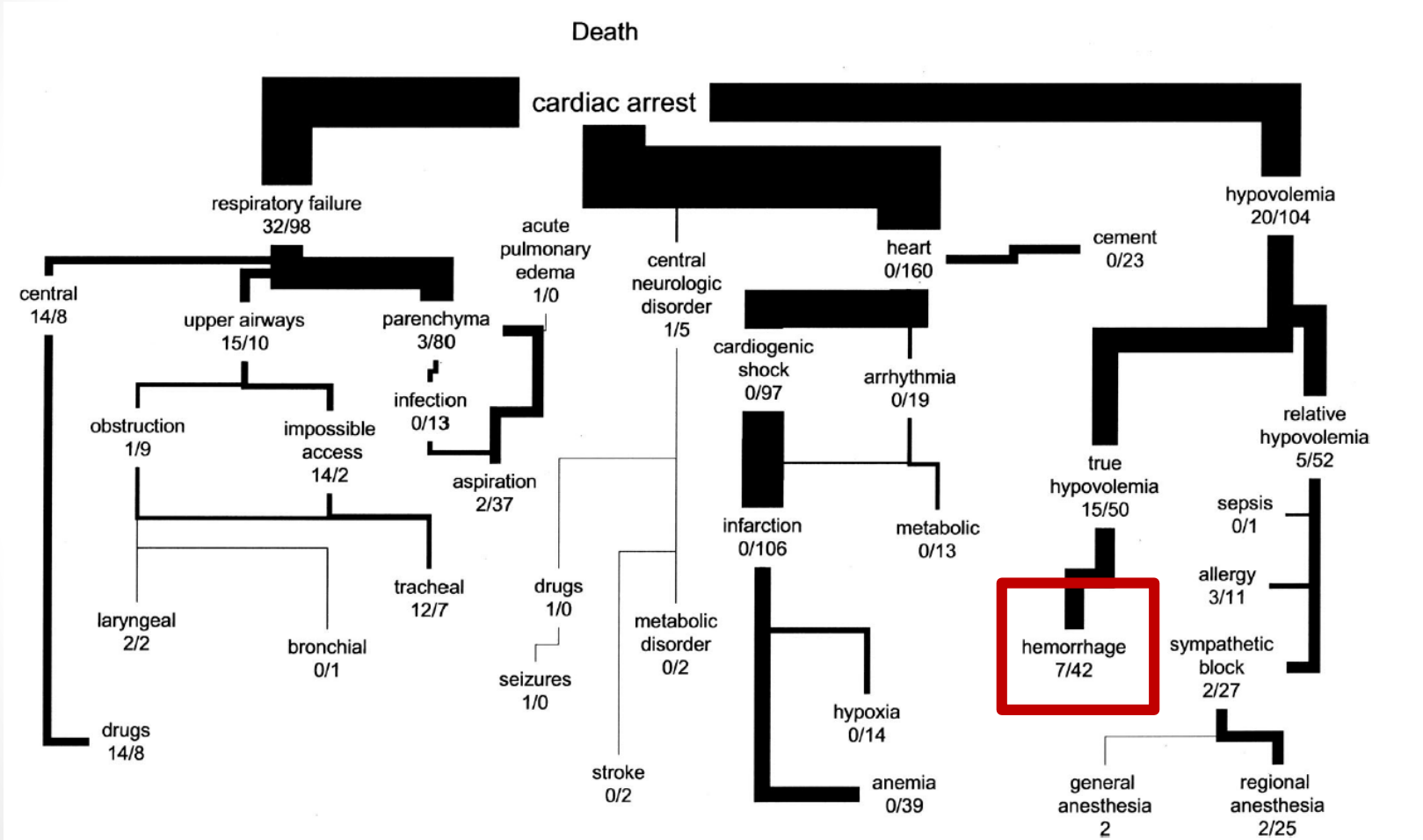

Fig. 4. Pathophysiologic description ("tree") of main events leading to deaths totally and partially related to anesthesia. The width of each line indicates the relative contribution of a given mechanism (number of cases totally related/partially related to anesthesia).

Anesthesiology, V 105, No 6, Dec 2006

Une physiopathologie complexe

- Choc Hypovolémique : hypoxie cellulaire et risque de mortalité … à court terme

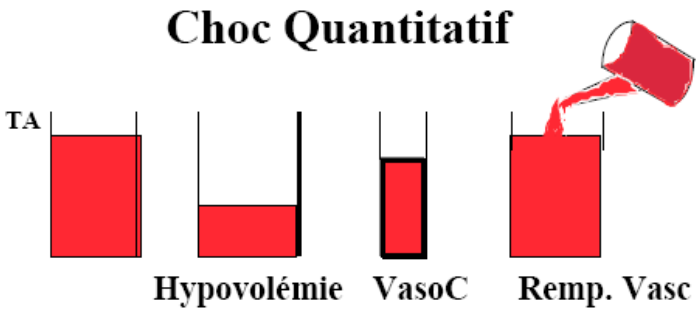

- Réponse Adaptative (mal-adaptative?) :
  - Volume et rapidité de l'hémorragie, Mécanismes compensateurs, Durée du choc, Lésions associées
  - Composante Redistributive, Inflammation, Reperfusion, Défaillance Multiviscérale, Transfusion …

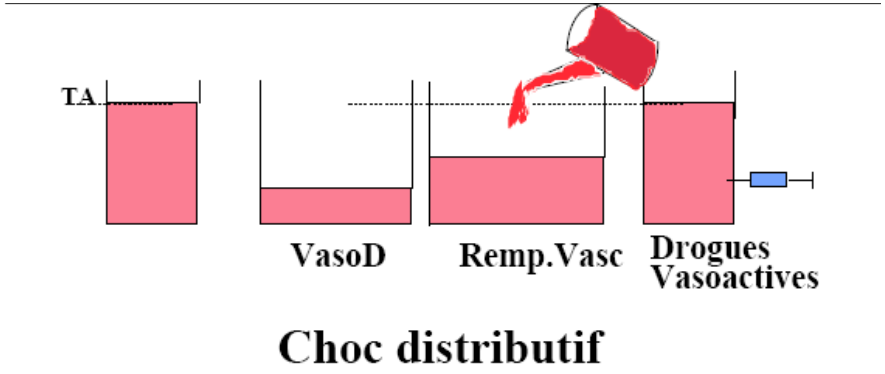

Hémorragie Progressive

- **1 Phase sympatho-excitatrice:**
  - Maintien PA
  - SN∑, SRA, AVP
  - Redistribution des flux

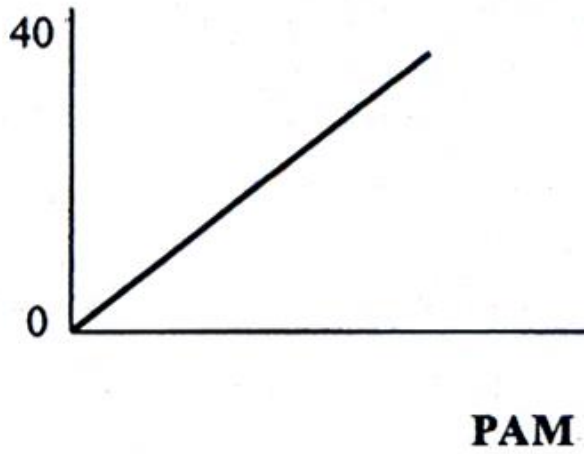

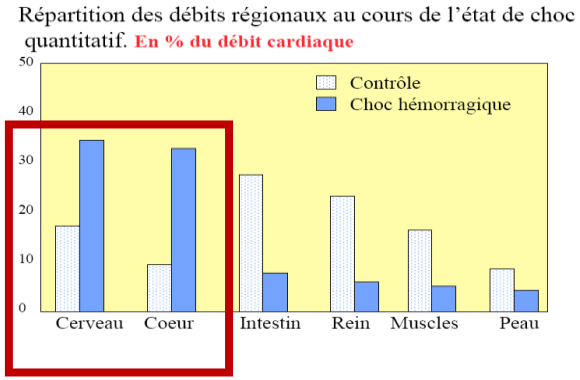

- **2 Phase sympatho-inhibitrice :**
  - Chute brutale PA
  - 30 à 50 % de la masse sanguine
  - bradycardie par libération du tonus vagal
  - Sympatholyse centrale et vasodilatation périphérique

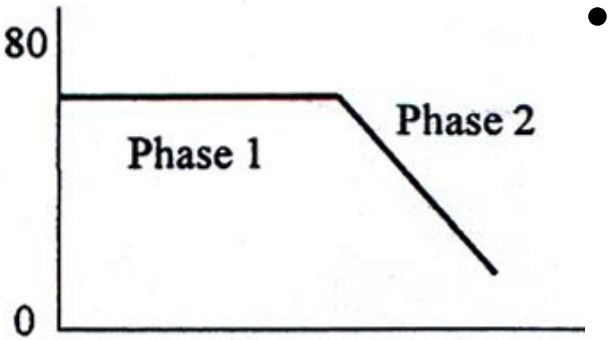

Évaluation *in vivo* de l'efficacité d'oxygénation tissulaire d'une émulsion de perfluorocarbure de nouvelle génération en situation de choc hémorragique

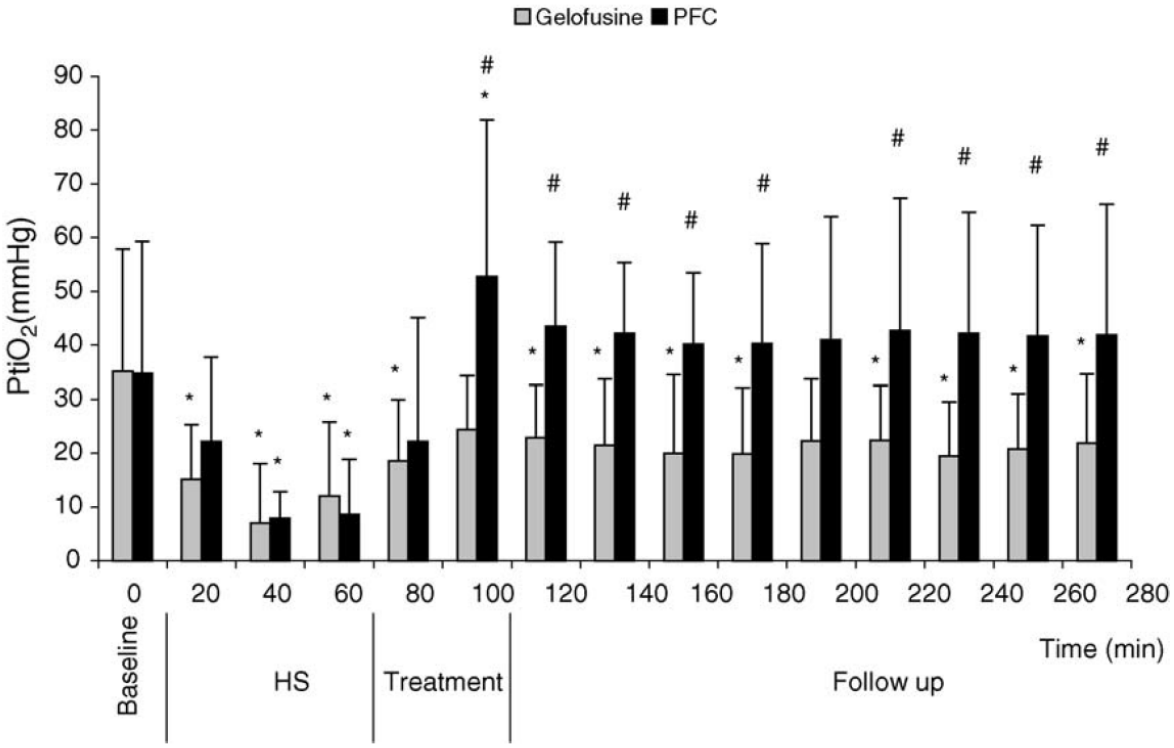

Figure 1 Time-dependent changes of skeletal muscular tissue oxygen pressure ($PtiO_2$) before and after HS, and after resuscitation with PFC emulsion ($n = 10$) or Gelofusine® ($n = 10$). Values are mean ± S.D. $^{*}p < 0.05$ vs. baseline, $^{\#}p < 0.05$ vs. Gelofusine®.

Audonnet, Mertes et al, Resuscitation (2006) 70, 124—132

Hémorragie et Hypotension « constante »

Schlumberger et al, Br J Anaesth, 74, 42, 1995

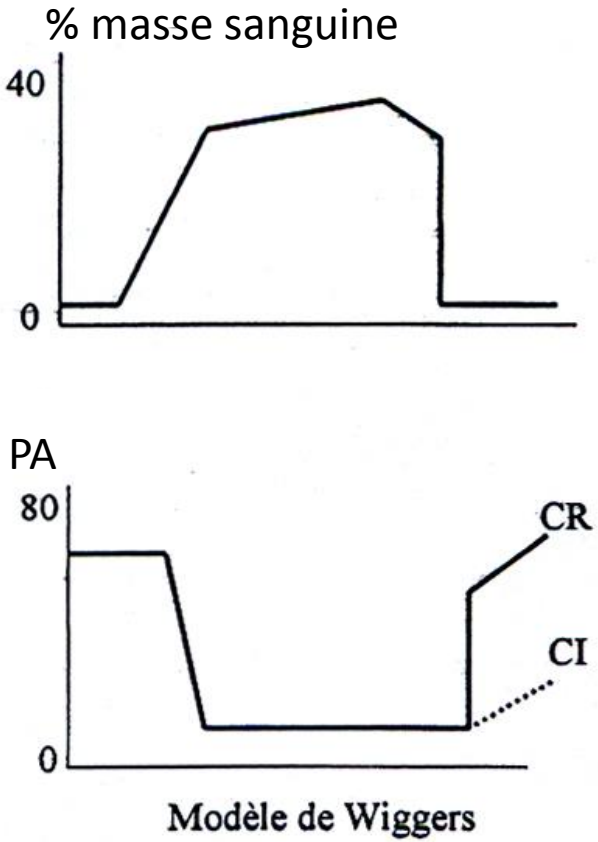

Choc prolongé :

- **vasodilatation**
- **perte de l'hystérésis**

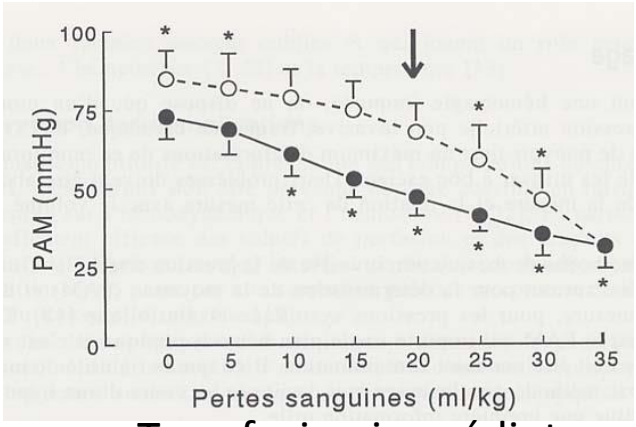

Transfusion immédiate

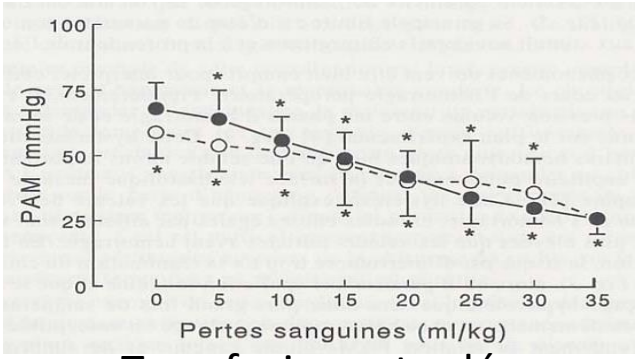

Transfusion retardée

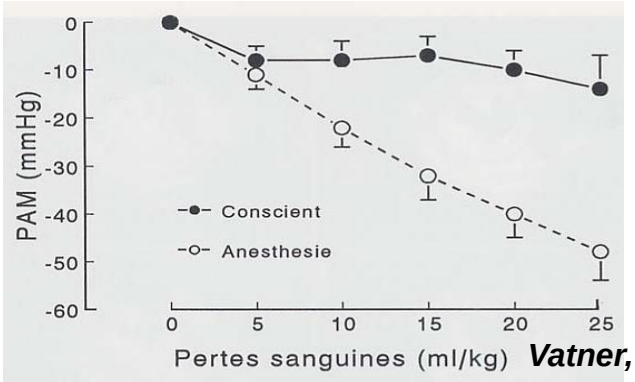

Vatner, NEJM, 293, 970, 1975

Conséquences métaboliques et inflammatoires

Hemorrhagic shock

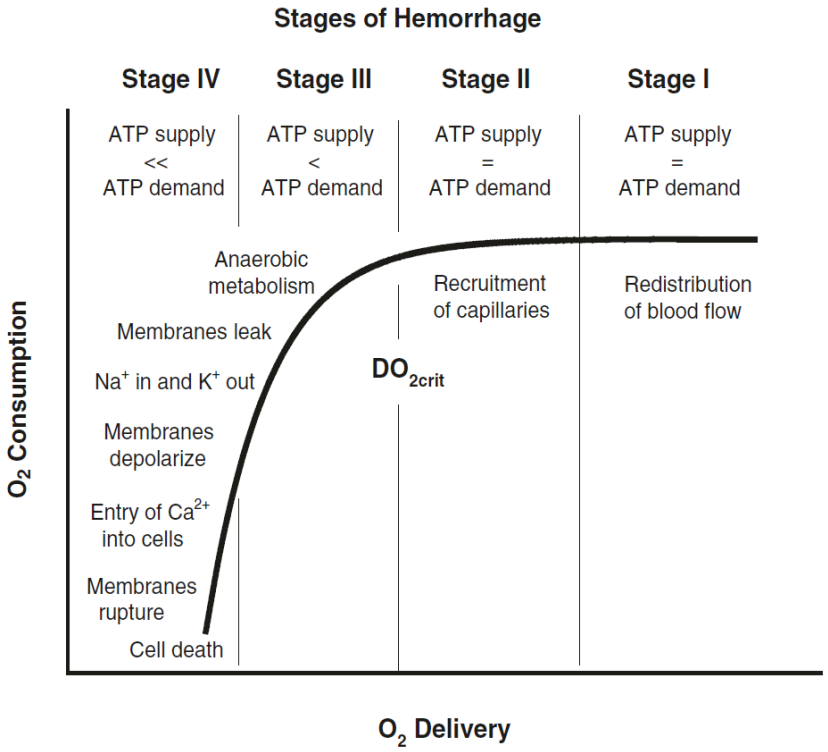

La concentration en O_2 (Co_2 ml/100 ml)

$Co_2 = Hb \times 1.34 \times SaO_2 + PaO_2 \times 0.003$

$CaO_2 = 20$ ml/100 ml

$CvO_2 = 15$ ml/100 ml

Le transport de l'O_2 (TO_2 ml/min/m_)

$TO_2 = CaO_2 \times Ic \times 10$

n = 660 ml/min/m_

La consommation d'O_2 (VO_2 ml/min/m_)

$VO2 = C (a - v) O_2 . IC$

n = 135 ml/min/m_

L'extraction de l'O_2 (O_2ER %)

$O_2ER = VO_2 / TO_2 = (CaO_2 – CvO_2) / CaO_2$

n = 25%

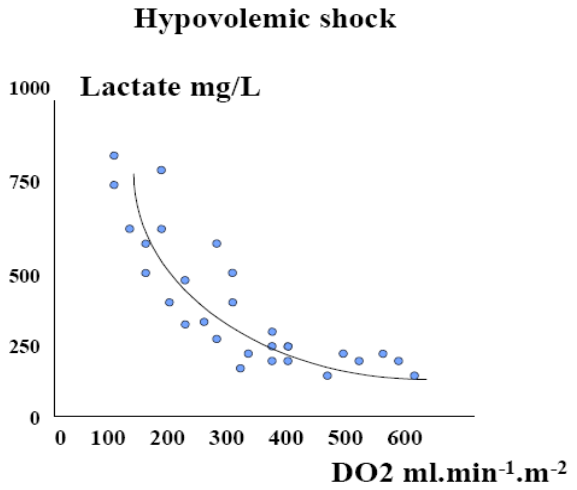

Groeneveld, Circ Shock , 1987, 22, 35-53

Critical Care October 2004 Vol 8 No 5 Gutierrez et al.

Alteration of cytokine profile following hemorrhagic shock

Cytokine 81 (2016) 35–38

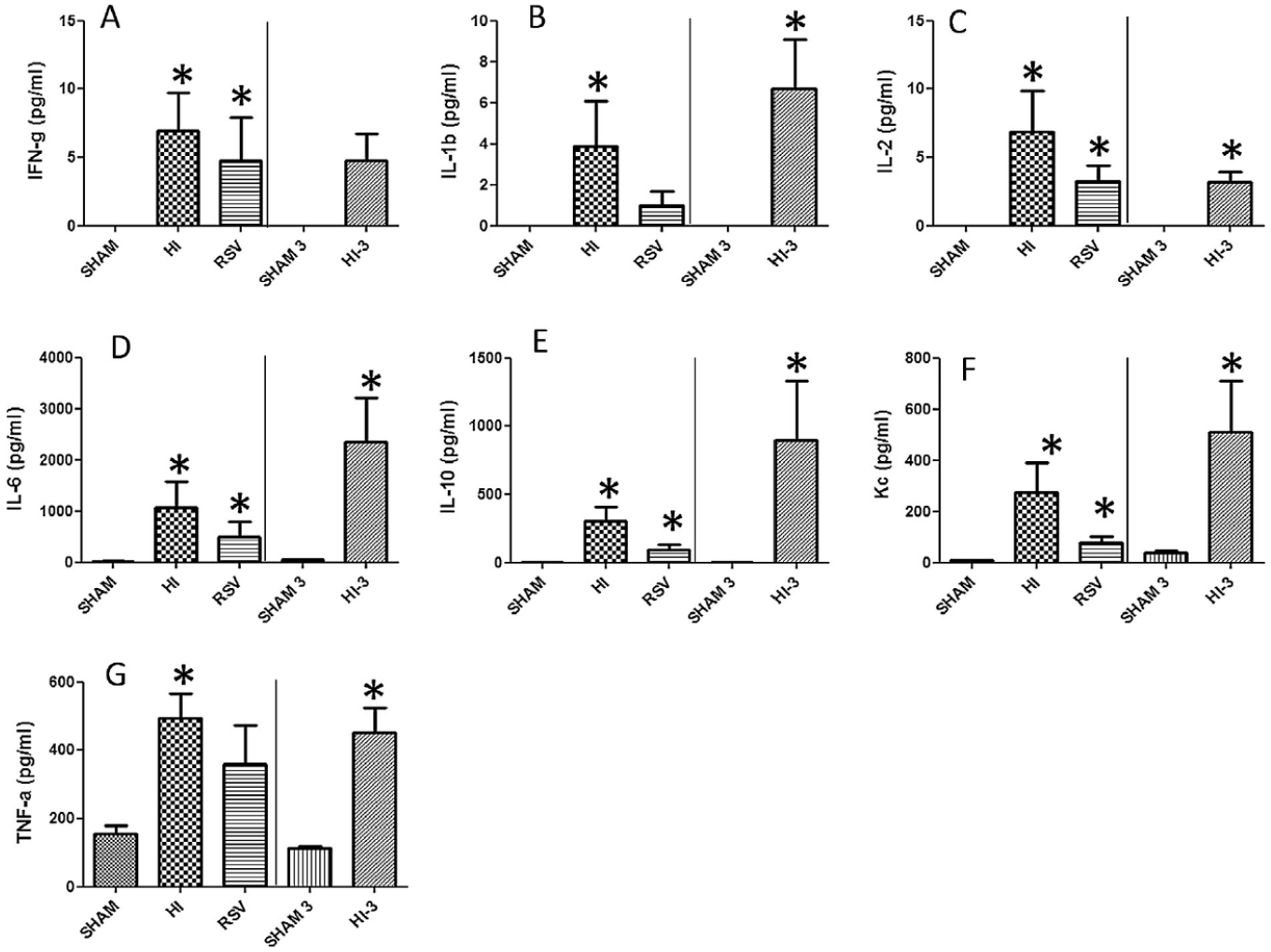

Fig. 2. Plasma cytokine profile following HI. Plasma cytokine profiles were determined using a multiplex method in sham, HI and RSV groups at 2 h followin resuscitation; or sham and HI (sham-3 and HI-3) at 3 h following HI and resuscitation. Values represent average of duplicates. $n = 6$ in each group; $^{*}p < 0.05$; bars mean ± SEM.

Patterns of gene expression among murine models of hemorrhagic shock/trauma and sepsis

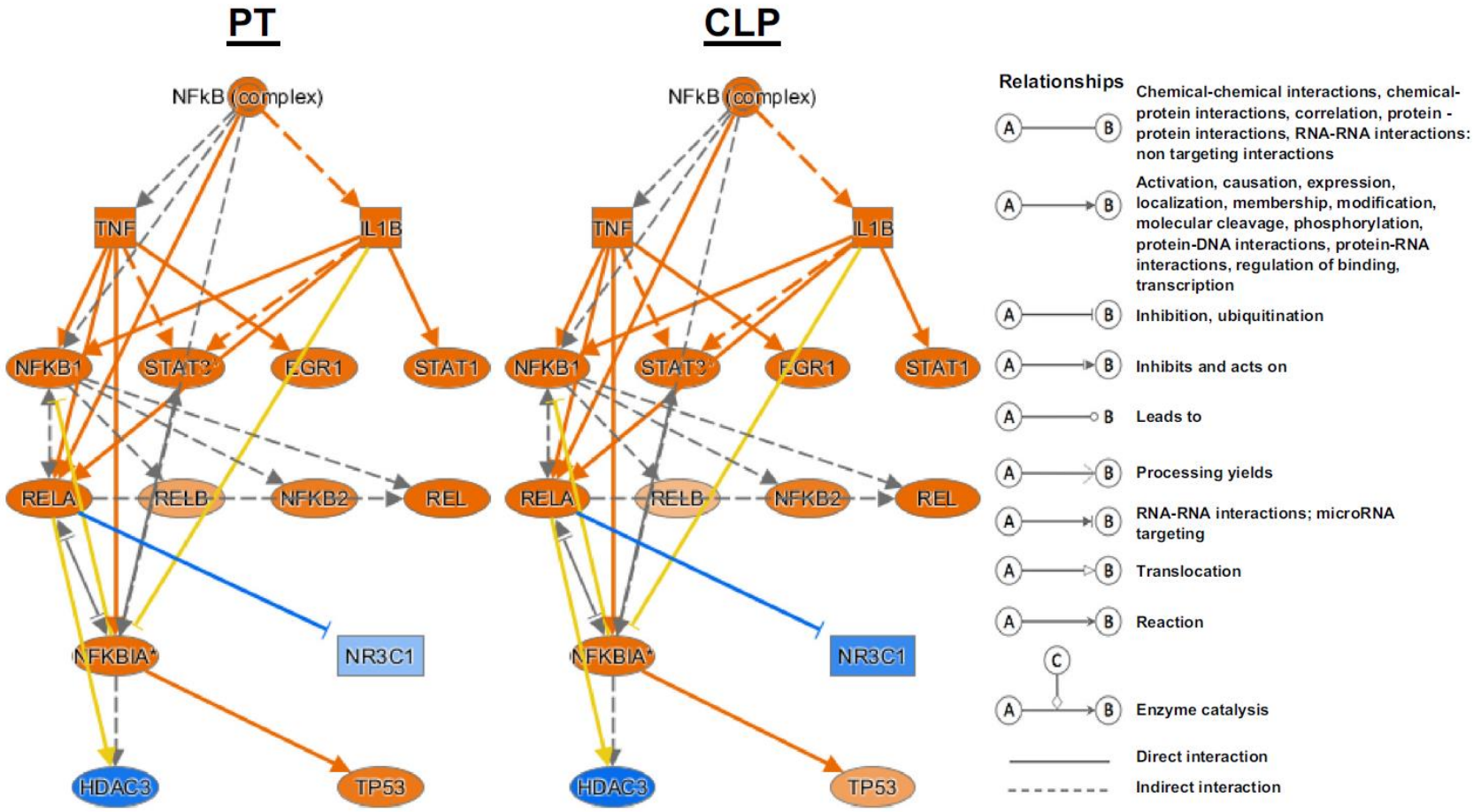

Fig. 7. Ingenuity Pathway Analysis (IPA) illustration showing upstream regulation of the pathway for NF-κB. The response to injury in both models at 2 h creates a very similar response. Orange, upregulation; blue, downregulation.

Physiol Genomics 48: 135–144, 2016.

The role of toll-like receptor-4 in the development of multi-organ failure following traumatic haemorrhagic shock and resuscitation

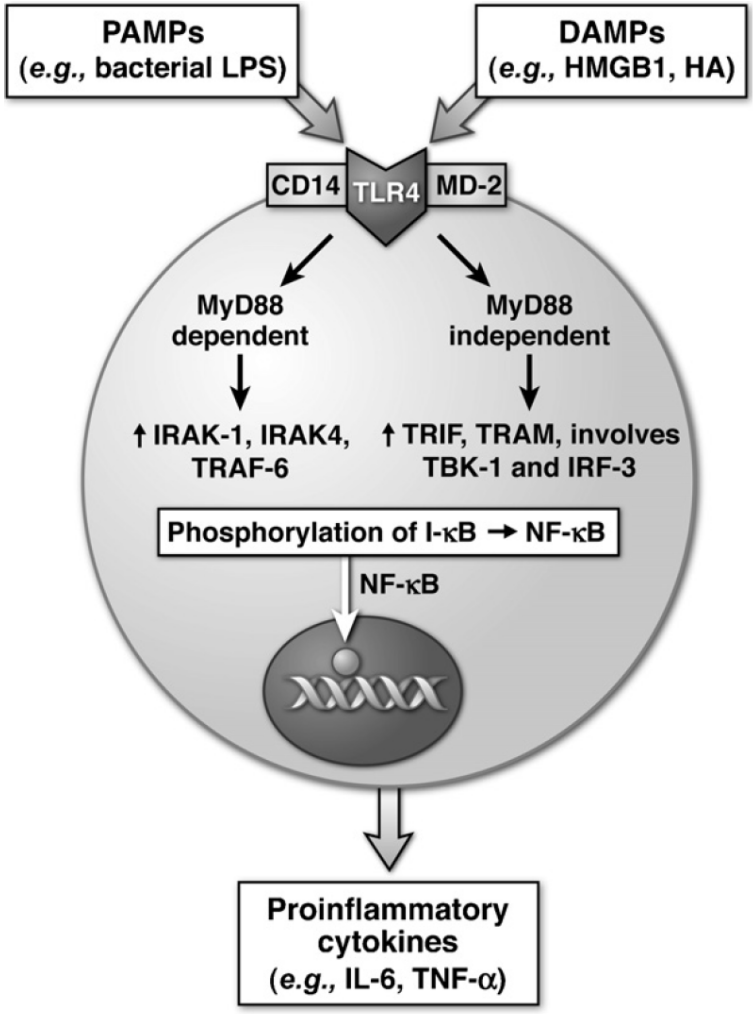

Fig. 1. Mechanism of activation of TLR4 and downstream signalling.

Injury, Int. J. Care Injured 43 (2012) 129–136

Protective role of nuclear factor erythroid 2-related factor 2 in the hemorrhagic shock-induced inflammatory response

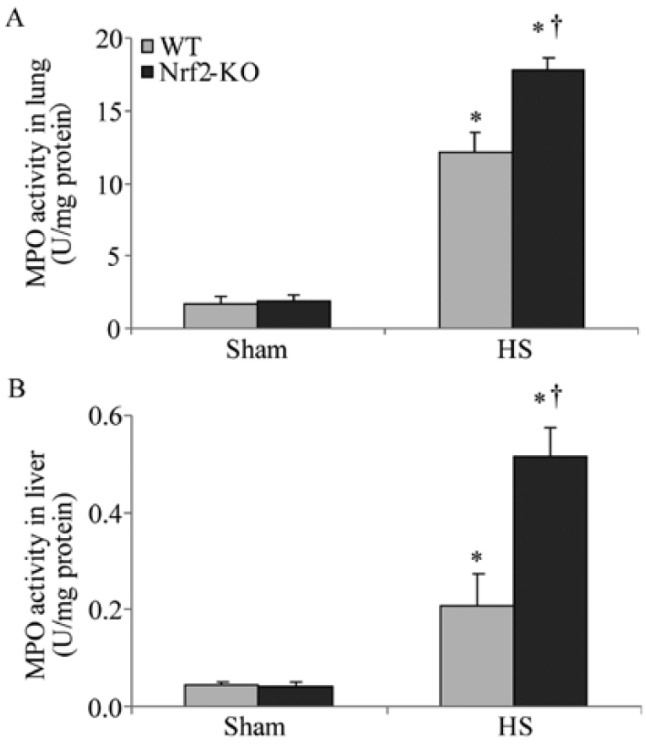

Figure 4. Higher myeloperoxidase (MPO) activity in lungs and livers of nuclear factor erythroid 2-related factor 2 (Nrf2)-KO mice subjected to hemorrhagic shock (HS). MPO activity was assessed as enzyme activity in tissue protein of (A) lung and (B) liver samples 2 h after HS. Data shown are the means ± SEM (n≥4 samples per group). *p<0.05 vs. sham-operated group (sham); †p<0.05 vs. WT mice.

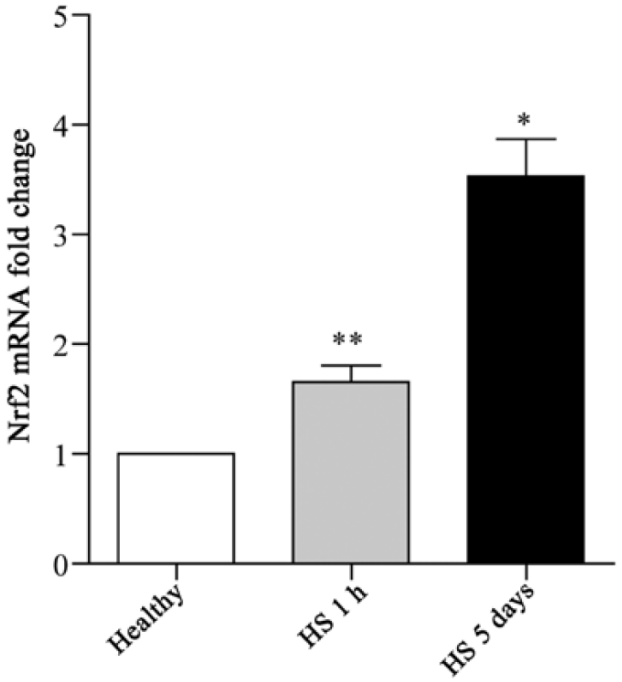

Figure 1. Marked induction of nuclear factor erythroid 2-related factor 2 (Nrf2) in leukocytes isolated from patients with hemorrhagic shock (HS). Whole blood samples were collected from healthy donors and patients with surgical-associated hemorrhage subjected to resuscitation treatment after 1 h or 5 days. White blood cells were subsequently isolated from these clinical samples and the transcript levels of Nrf2 were then quantified by RT-qPCR. Data shown are the means ± SEM from 6 samples per group. *p<0.05 vs. healthy donor samples, **p<0.001 vs. healthy donor samples.

INTERNATIONAL JOURNAL OF MOLECULAR MEDICINE 37: 1014-1022, 2016

Défaillances Multivsicérales

Neurohormonal interactions on the renal oxygen delivery and consumption in haemorrhagic shock-induced acute kidney injury

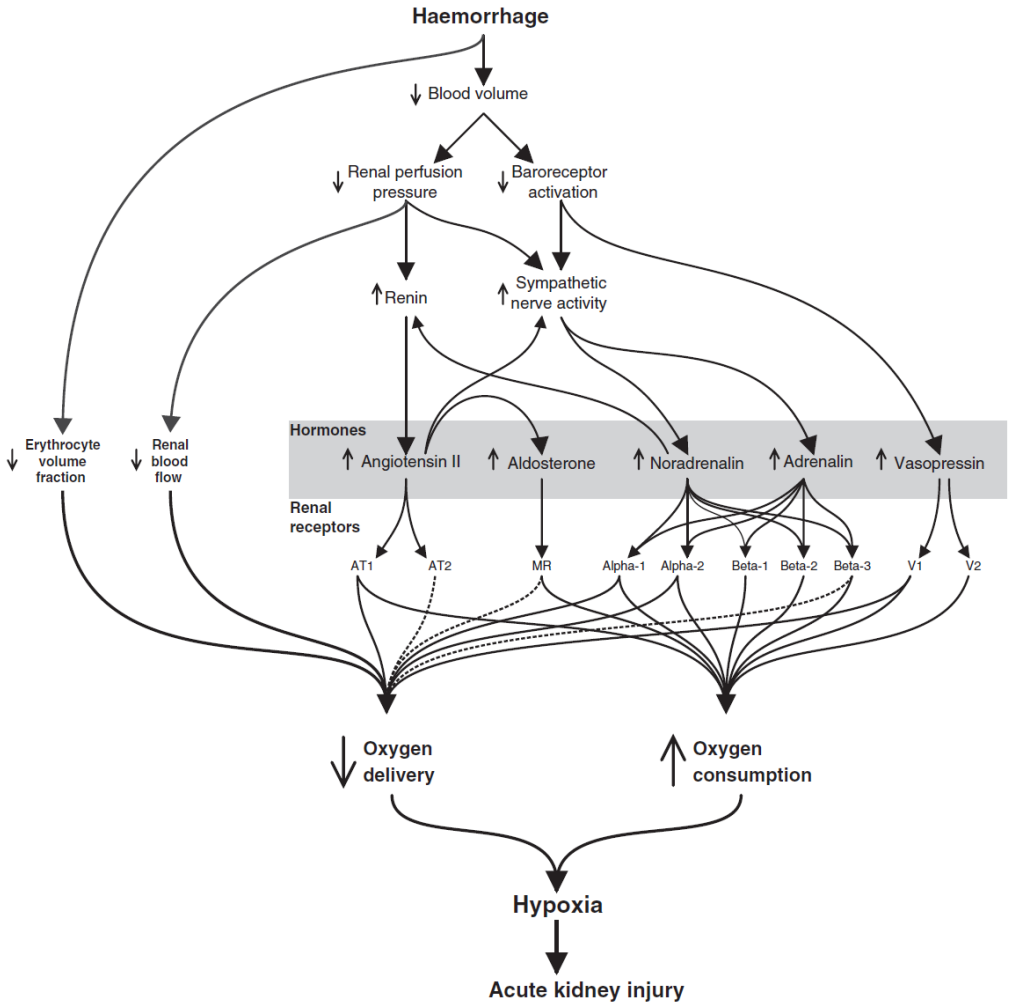

Figure 2 Haemorrhage affects renal oxygenation by a variety of mechanisms. The two more direct effects are the reduced oxygen-carrying capacity of blood caused by the reduction in erythrocyte volume fraction and the reduced renal perfusion pressure. In addition, the reduced blood volume activates neurohormonal signalling through the renin–angiotensin–aldosterone system, the sympathetic nervous system and vasopressin to increase peripheral resistance and fluid retention in order to maintain perfusion to the central organs. This is unfortunate for the kidneys that both require a large blood flow and do the bulk of fluid retention using active reabsorption. Thus, both oxygen delivery and oxygen consumption are affected and increase the susceptibility of the kidney to acute kidney injury (AKI) in haemorrhagic shock.

Acta Physiol 2013, 209, 11–25

Microcirculatory Alterations in Traumatic Hemorrhagic Shock

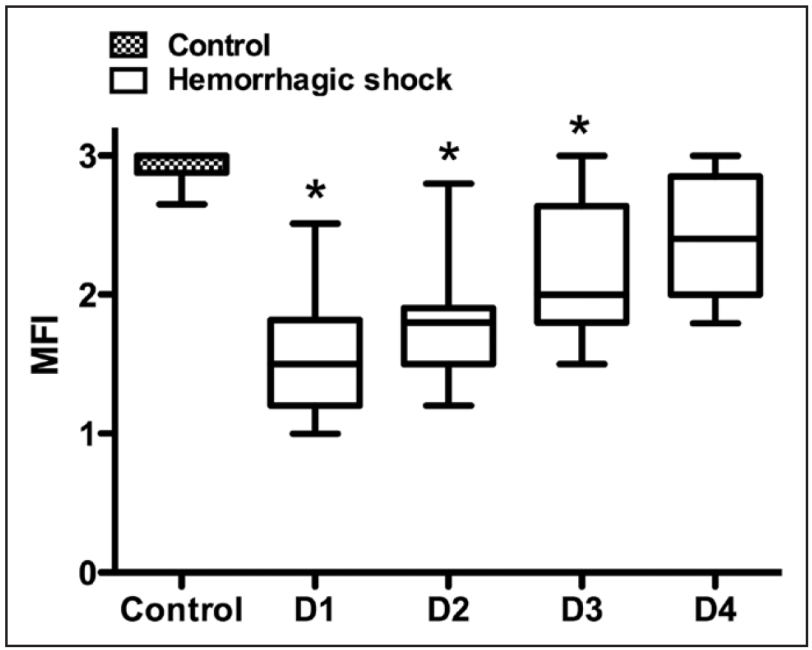

Figure 1. Microcirculatory flow index (MFI) at D1, D2, D3, and D4. *$p < 0.05$ versus control.

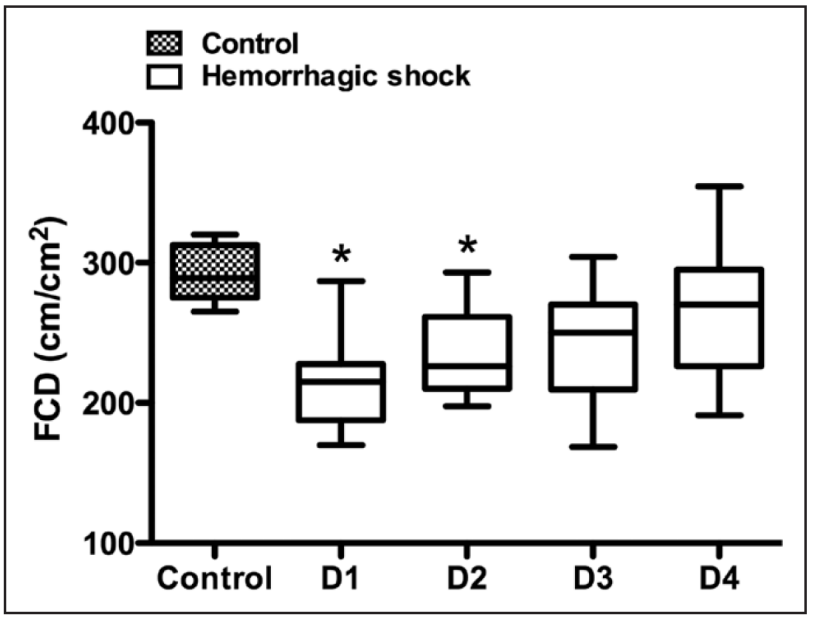

Figure 3. Functional capillary density (FCD) (cm/cm^{-2}) at D1, D2, D3, and D4. *$p < 0.05$ versus control.

Tachon et al, Crit Care Med 2014; 42:1433–1441)

In vivo analysis of intestinal permeability following hemorrhagic shock

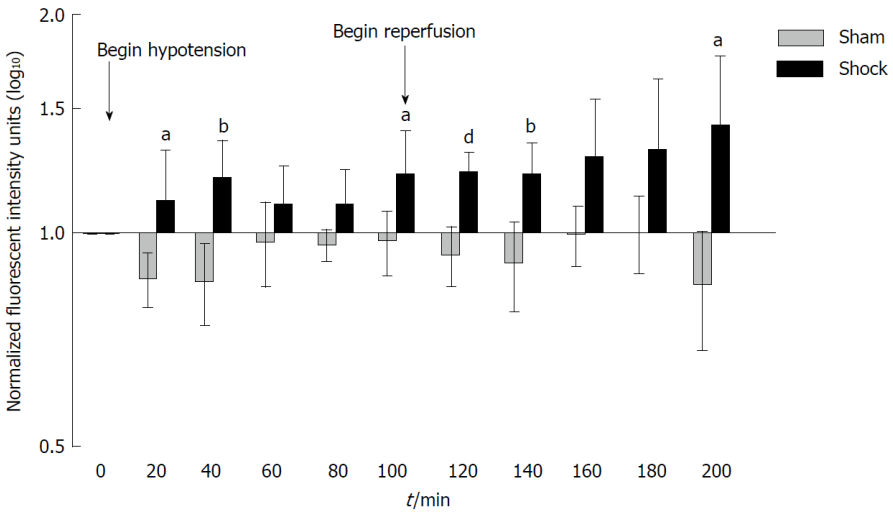

Increased bowel permeability to casein peptides after hemorrhagic shock. Small bowel permeability as measured by systemic concentrations of proteolytically-generated peptides from fluorescently labelled casein injected into the small bowel. Note the early increase in bowel permeability at 20 min, followed by a second, sustained increase in bowel permeability at reperfusion.

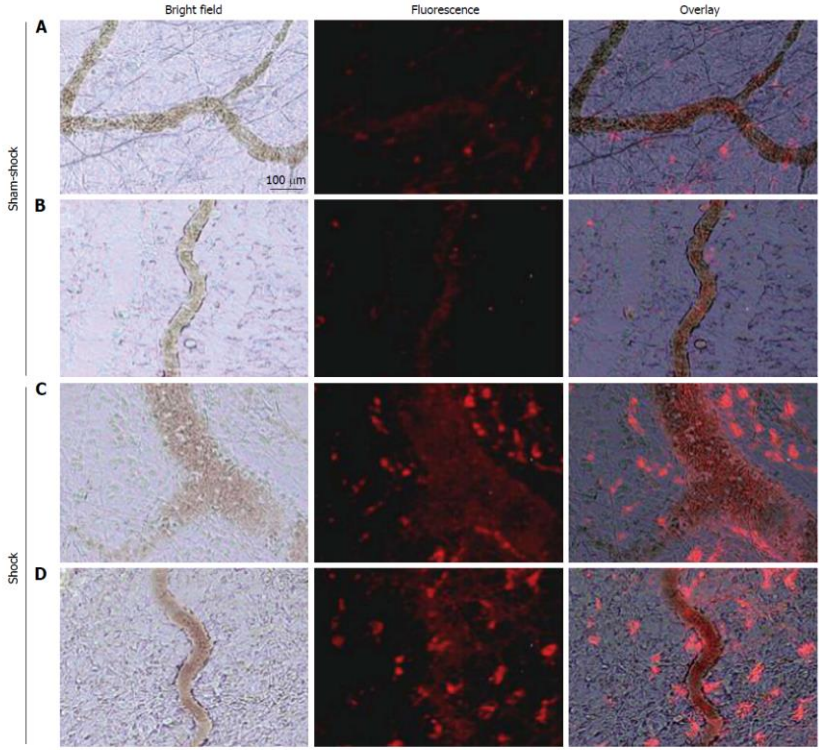

Selected *in vivo* microvascular images from two different sham-shock control (A and B) and shock (C and D) animals (*n* = 6, both groups) after hemorrhagic shock or sham-shock and reperfusion. Note the significantly higher levels of red fluorescent casein-derived peptides in the microvasculature and within the interstitium in shock animals (C and D) compared with their sham shock counterparts (A and B).

World J Crit Care Med. Nov 4, 2015; 4(4): 287-295

The Role of Intrinsic Apoptotic Signaling in Hemorrhagic Shock-Induced Microvascular Endothelial Cell Barrier Dysfunction

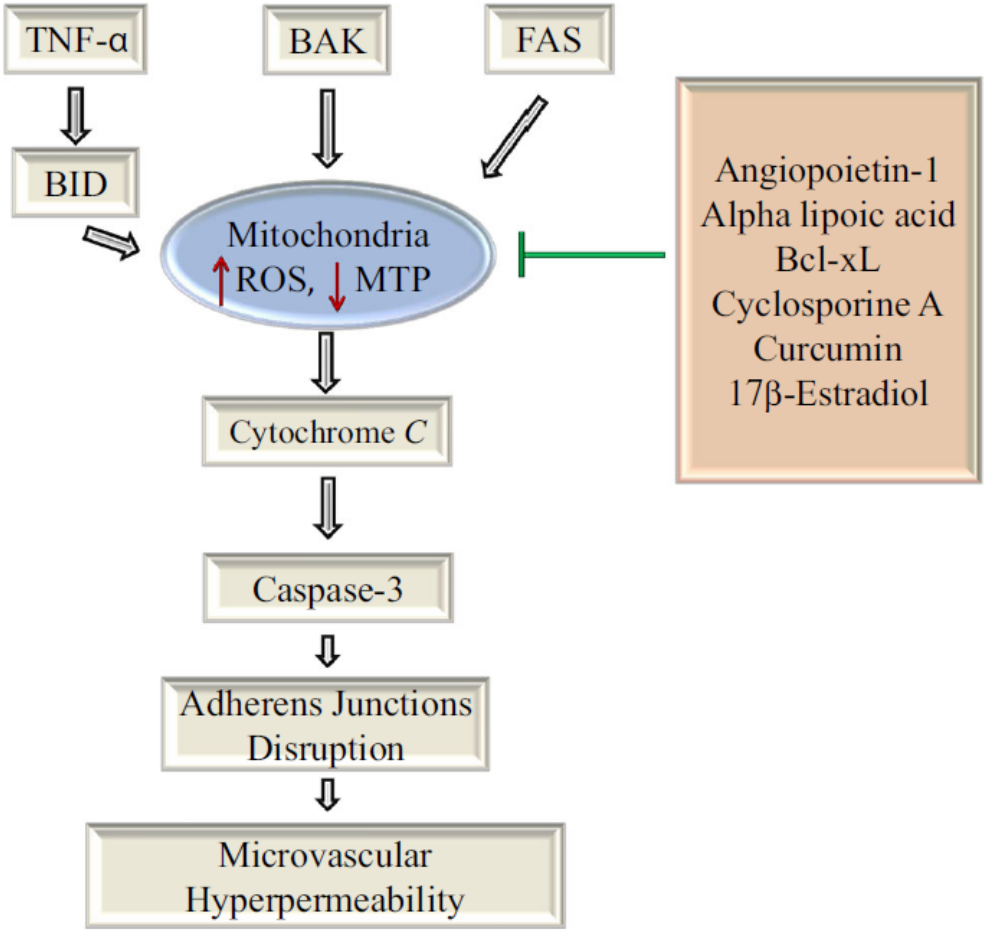

Pro-apoptotic proteins such as BAK, TNF-α, and Fas initiate mitochondria-mediated intrinsic apoptotic signaling, resulting in increase in reactive oxygen species (ROS) formation, decrease in mitochondrial transmembrane potential (MTP), and release of cytochrome c from mitochondria. The cytochrome c, in turn, activates the final effector caspase-3 in the apoptotic pathway. The active caspase-3 then disrupts the endothelial cell adherens junction protein complex, leading to increase in microvascular permeability.

J. of Cardiovasc. Trans. Res. (2014) 7:711–718

A “clean case” of systemic injury: Mesenteric lymph after hemorrhagic shock elicits a sterile inflammatory response

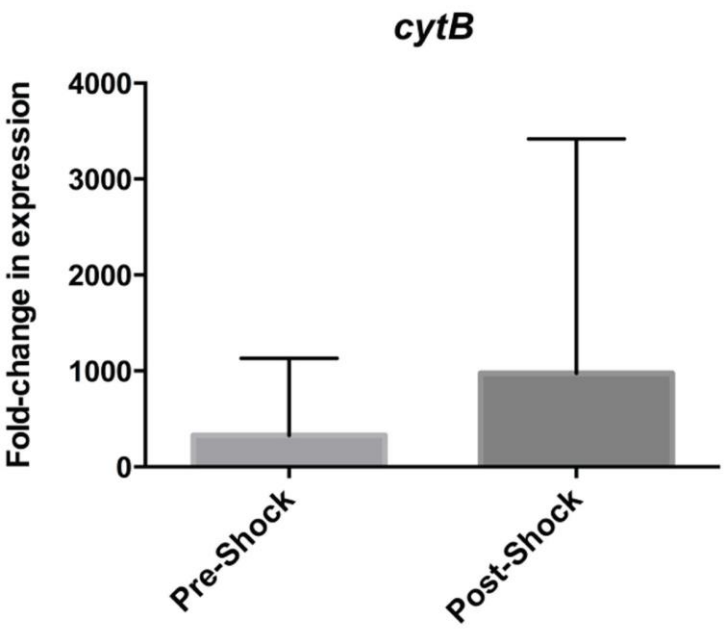

Figure 1.
Relative fold-change in expression of mitochondrial DAMPs *cytB* in pre-shock and post-shock mesenteric lymph as compared to the housekeeping gene *18s*.

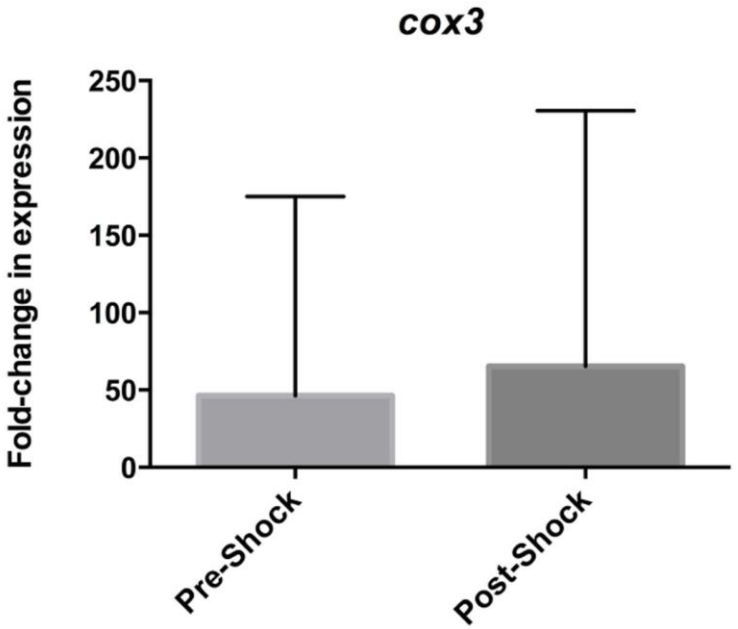

Figure 2.
Relative fold-change in expression of mitochondrial DAMPs *cox3* in pre-shock and post-shock mesenteric lymph as compared to the housekeeping gene *18s*.

Lymphe mésentérique : DAMPs +, Translocation -

Shock. 2015 October ; 44(4): 336–340.

Alveolar macrophage activation after trauma-hemorrhage and sepsis is dependent on NF-B and MAPK/ERK mechanisms

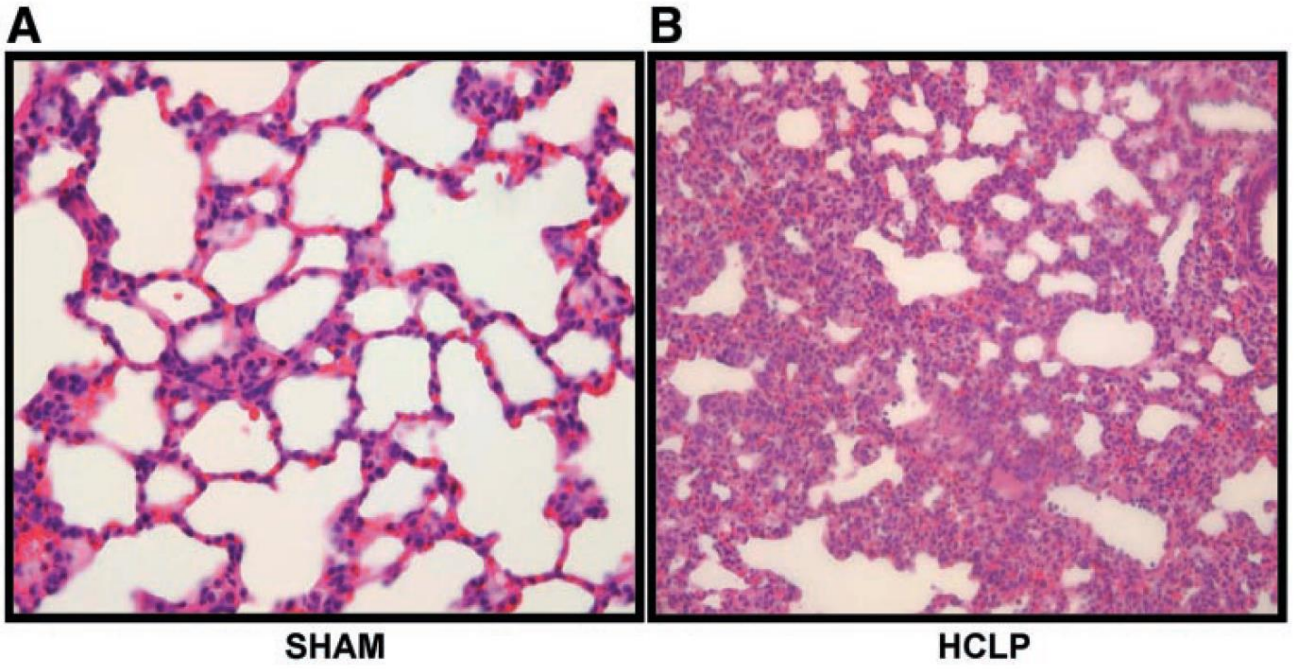

Fig. 4. In a separate group of animals, HCLP was induced as described in Fig 1. Lungs were harvested as described in MATERIALS AND METHODS and stained with hematoxylin and eosin. This figure shows the comparison between a sham-operated animal and one animal from the experimental group. Whereas in the control group, normal lung architecture is seen, the lung tissues after HCLP are characterized by neutrophil influx, edema, and wall thickening.

Am J Physiol Lung Cell Mol Physiol 283: L799–L805, 2002;

The role of toll-like receptor-4 in the development of multi-organ failure following traumatic haemorrhagic shock and resuscitation

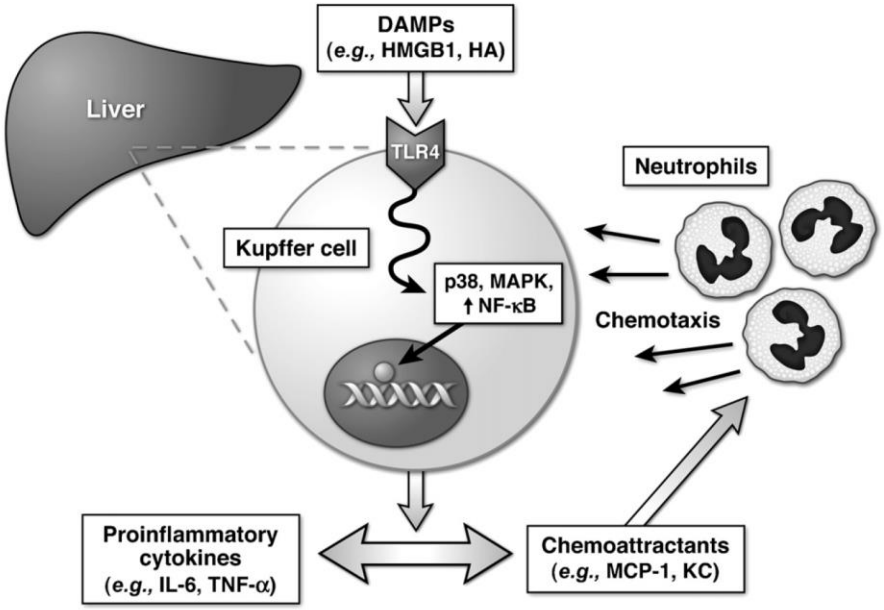

Fig. 2. The role of Kupffer cells in TLR4-mediated hepatic inflammation.

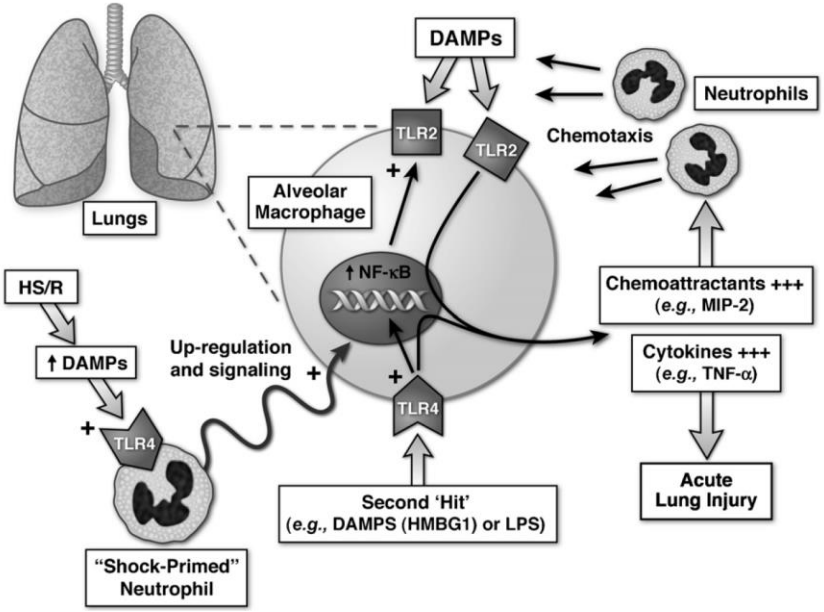

Fig. 3. Upregulation of TLR2 in TLR4-mediated acute lung injury: the "two-hit" hypothesis.

Injury, Int. J. Care Injured 43 (2012) 129–136

Coagulopathy

Coagulopathy: Its Pathophysiology and Treatment in the Injured Patient

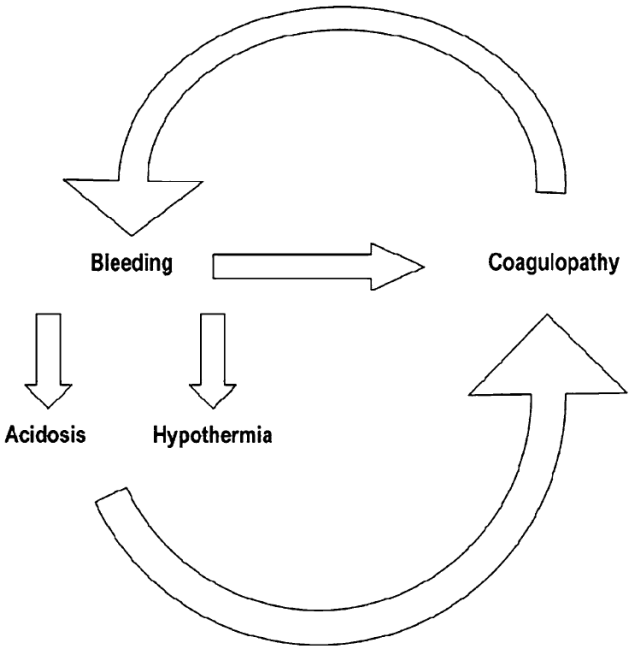

Figure 1. Depiction of lethal triad. Blood loss leads to acidosis and hypothermia resulting in coagulopathy that perpetuates further bleeding. Reprinted from Schreiber MA, Damage control surgery. Critical Care Clinics 20:101–118, 2004 with permission from Elsevier.

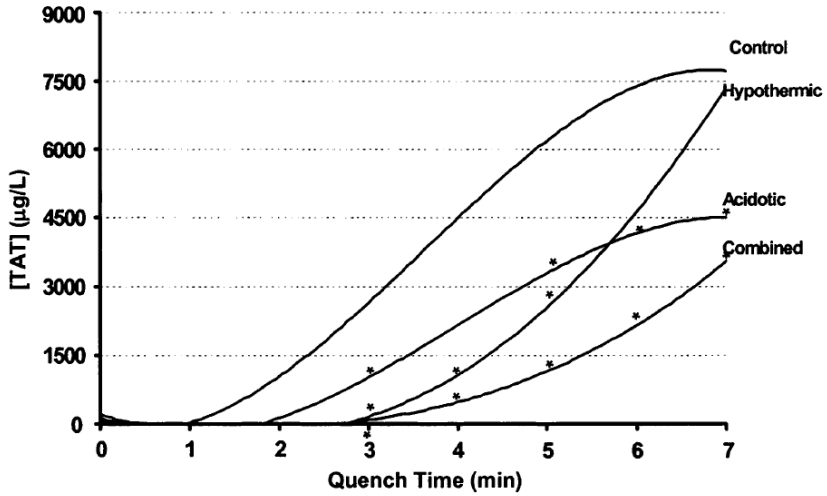

Figure 3. Thrombin generation rate in blood samples measured as thrombin-antithrombin III (TAT) complex concentration. The TAT concentration was measured in sample aliquots at time 0 (sample withdrawal) and at 1-min intervals thereafter to determine thrombin generation with time in each sample. $^{*}P < 0.05$, different from normal value at the same quench time point. Reprinted with permission from Martini WZ *et al.*, Independent contributions of hypothermia and acidosis to coagulopathy in swine. J Trauma 2005;58:1002–1010.

World J Surg (2007) 31: 1055–1064

Inflammatory response to trauma: Implications for coagulation and resuscitation

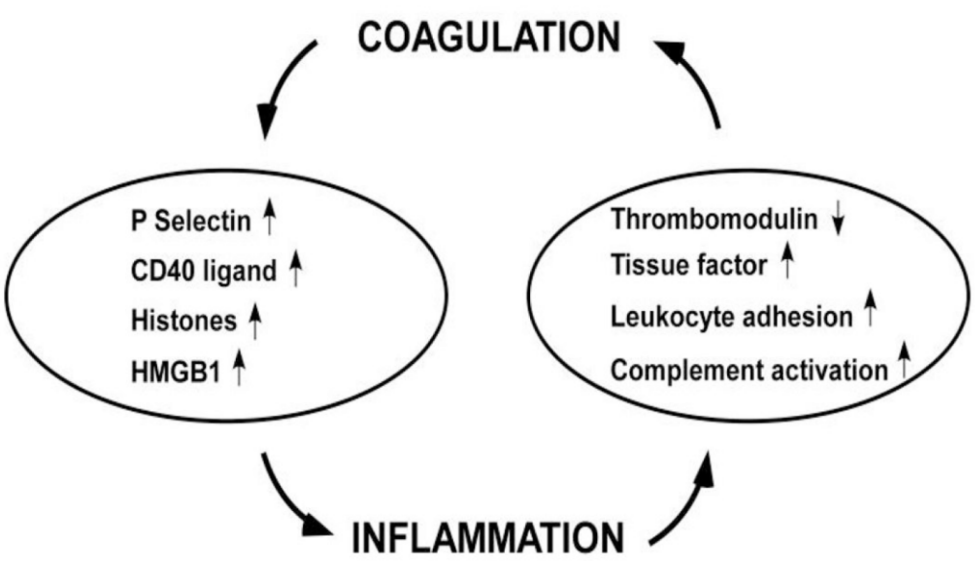

Figure 1. The impact of coagulation on inflammation and the impact of inflammation on coagulation

Coagulation triggers platelet activation and leads to P selectin and CD40 ligand expression platelet surface. Ischaemia leads to cell death and the release of histones and HMGB1, both of which augment inflammation. Inflammation in turn leads to tissue factor induction, leukocyte adhesion, thrombomodulin down regulation, and complement activation, Thus, coagulation increases inflammation that in turn increases coagulation. Adapted from (44).

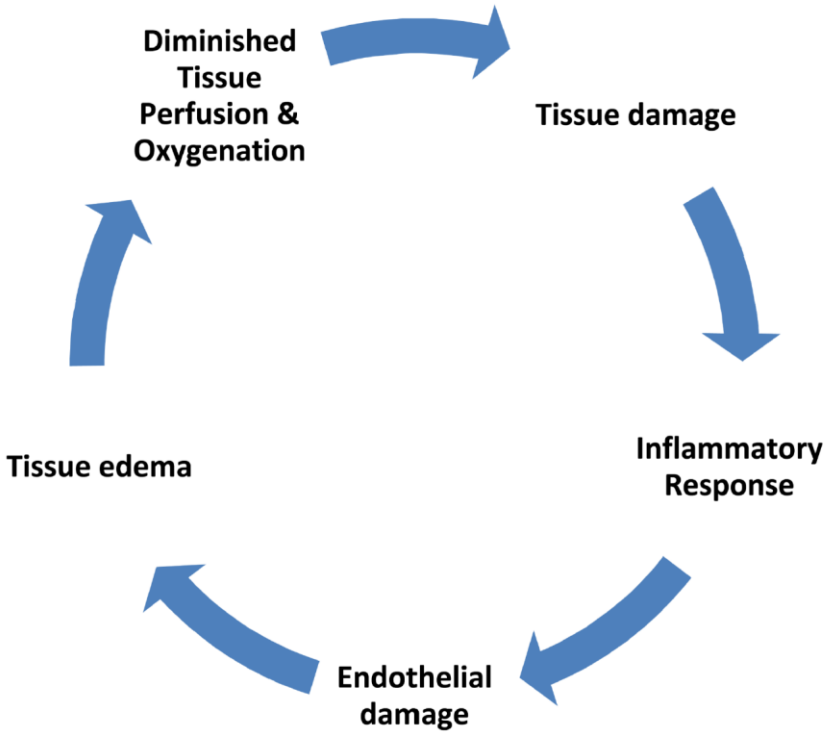

Figure 2. The vicious cycle of tissue damage and inflammatory response

Tissue damage causes a local inflammatory response that may become more systemic. This systemic inflammation leads to endothelial damage at distant sites (including the lungs). The resulting tissue edema, decreased microperfusion and tissue hypoxia leads to more tissue damage.

Curr Opin Anaesthesiol. 2014 April ; 27(2): 246–252

Inflammatory response to trauma: Implications for coagulation and resuscitation

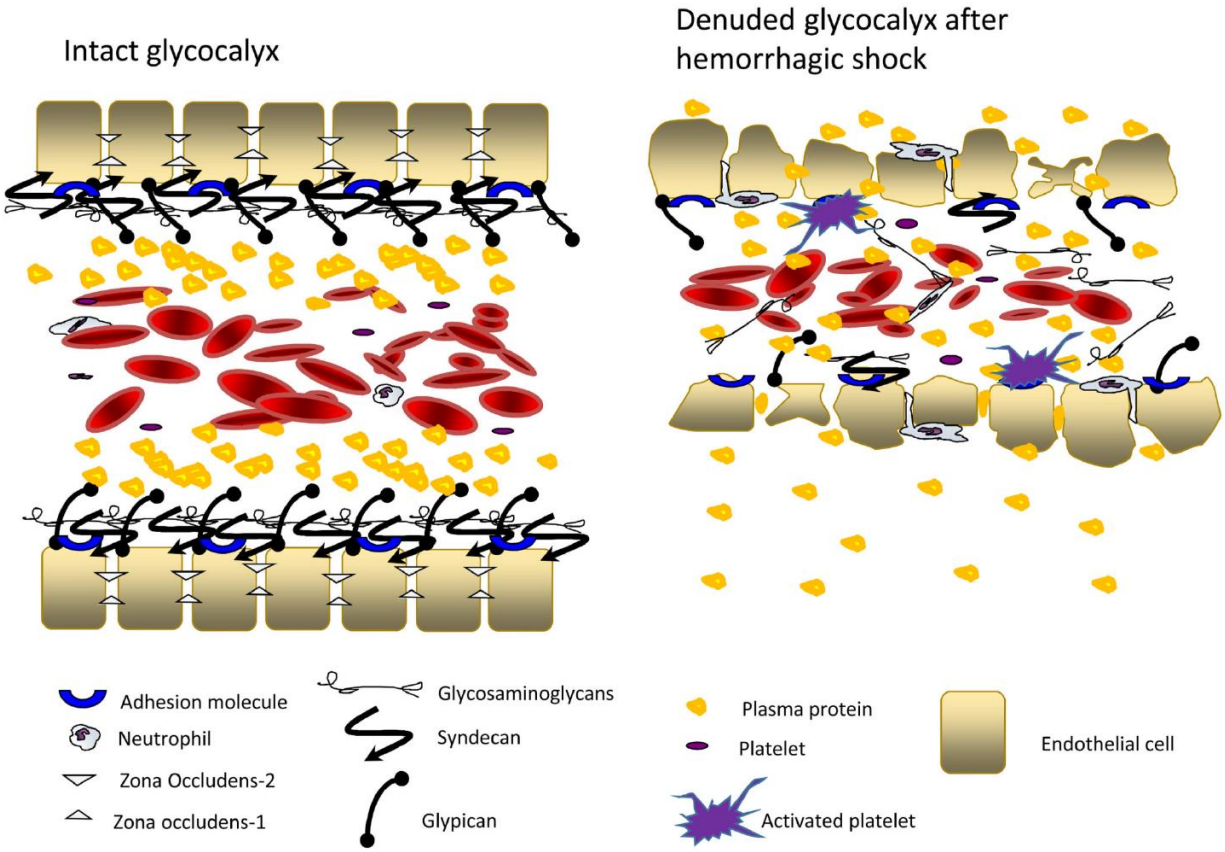

Figure 3. Endothelial glycocalyx damage associated with systemic inflammation
The normal functions of the Endothelial Surface Layer (ESL) to maintain homeostasis are lost when glycocalyx degradation occurs. Loss of plasma proteins and fluid to the interstitium, inappropriate activation of coagulation and immune competent cells all contribute to edema and microcirculatory compromise.

Curr Opin Anaesthesiol. 2014 April ; 27(2): 246–252

Characterization of platelet dysfunction after trauma

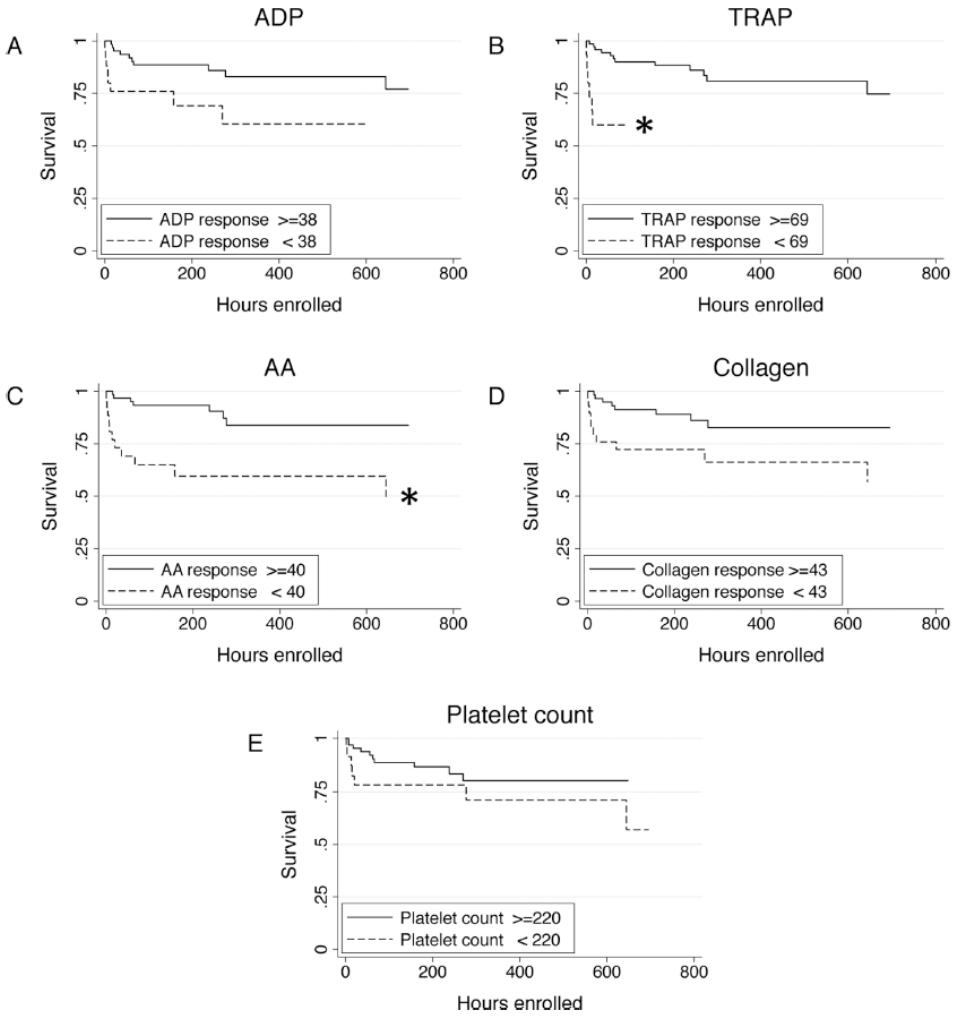

Figure 3.
Kaplan-Meier 30-day survival curves showing survival differences between patients with below-normal admission platelet responsiveness to adenosine diphosphate (ADP; a), thrombin receptor-activating peptide (TRAP; b), arachidonic acid (AA; c), and collagen (d). Survival curves for patient admission platelet counts below the 25th percentile (e) are shown for comparison. *$p < 0.05$ by log-rank test.

J Trauma Acute Care Surg. 2012 July ; 73(1): 13–19.

A time course study of acute traumatic coagulopathy prior to resuscitation: From hypercoagulation to hypocoagulation caused by hypoperfusion?

Transfusion and Apheresis Science 50 (2014) 399–406

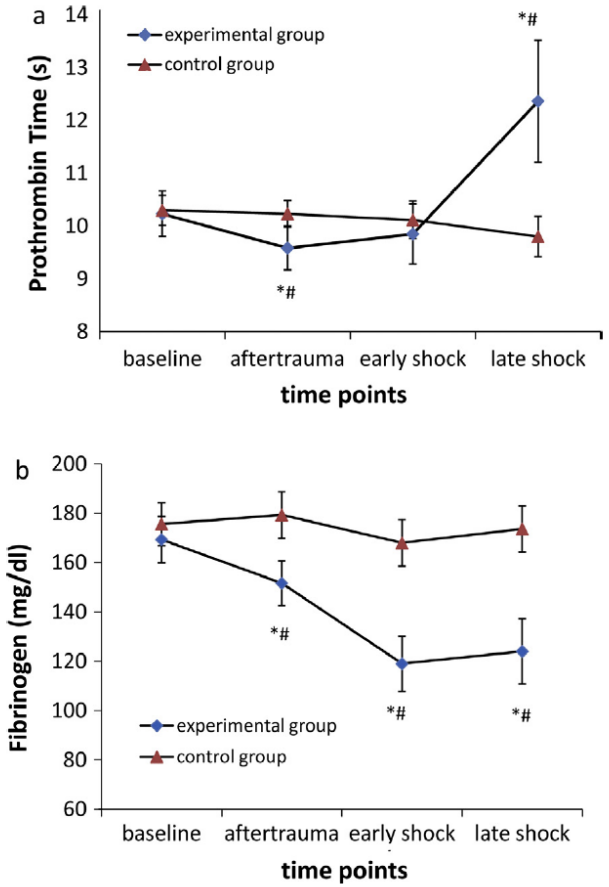

Fig. 2. The changes of PT and fibrinogen concentration during trauma and hemorrhagic shock (mean ± SE). After trauma, early shock and late shock represent 5 min after multi-trauma, 10 min after shock and 40 min after shock respectively. Experimental group $n = 12$, control group $n = 6$. (a) PT alterations during the experiment. (b) Fibrinogen concentration alterations during the experiment. Significant data measured from baseline are labeled (*) with p-values <0.05. Significant data measured from corresponding control group are labeled (#) with p-values <0.05.

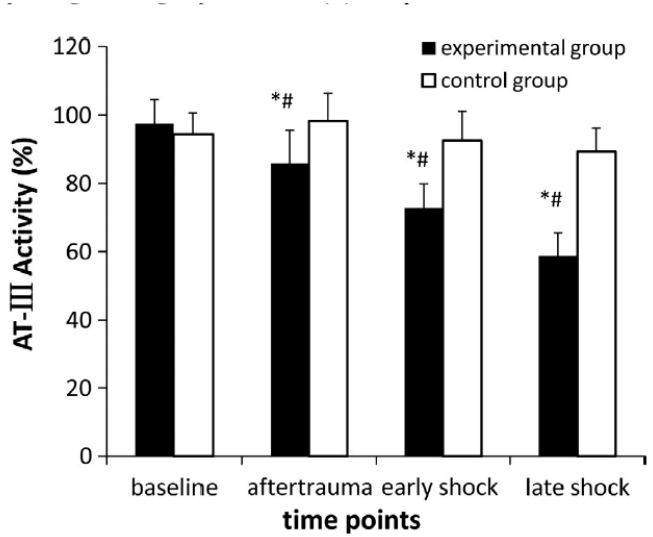

Fig. 3. The changes of AT-III during trauma and hemorrhagic shock (mean ± SE). After trauma, early shock and late shock represent 5 min after multi-trauma, 10 min after shock and 40 min after shock respectively. Experimental group $n = 12$, control group $n = 6$. Significant data measured from baseline are labeled (*) with p-values <0.05. Significant data measured from corresponding control group are labeled (#) with p-values <0.05.

Cellular microparticle and thrombogram phenotypes in the Prospective Observational Multicenter Major Trauma Transfusion (PROMMTT) Study: correlation with coagulopathy

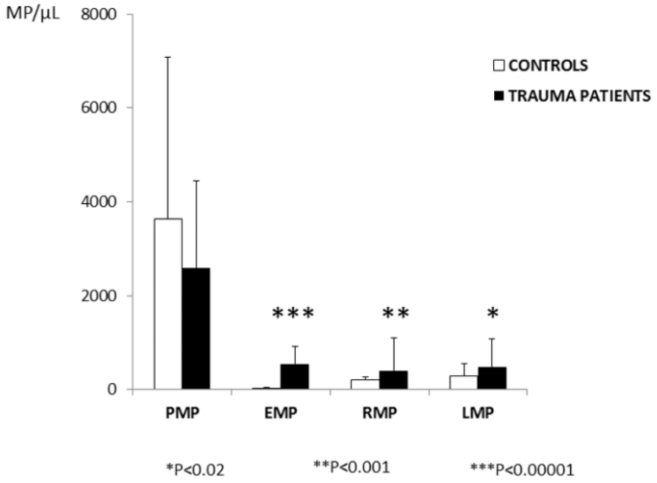

Figure 1. Microparticle Phenotypes in Controls and PROMMTT Trauma Patients
PMP=platelet microparticles; EMP=endothelial microparticles; RMP=red blood cell microparticles; LMP=leukocyte microparticles. *p<0.02, **p<0.001, ***p<0.00001.

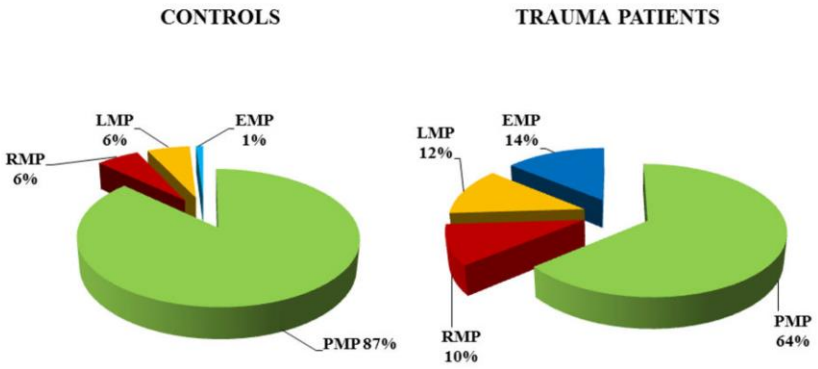

Figure 2. Microparticle Phenotypes Distribution in Controls and PROMMTT Trauma Patients
PMP=platelet microparticles; RMP=red blood cell microparticles; LMP=leukocyte microparticles; EMP=endothelial microparticles

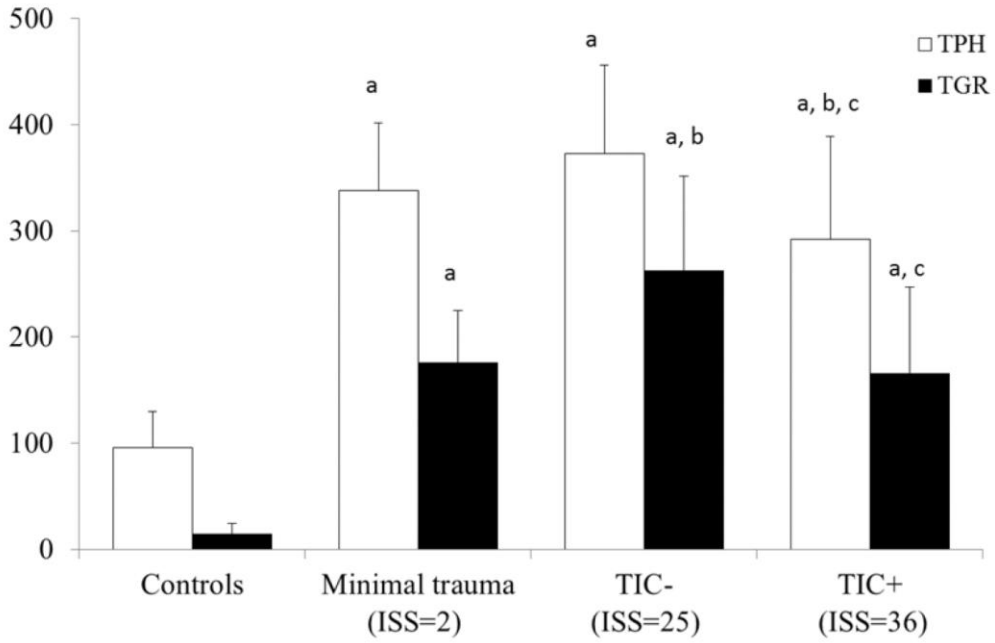

Figure 4. Thrombin Peak Height (TPH) and Thrombin Generation Rate (TGR) in Controls and Trauma Patients
TIC-=noncoagulopathic; TIC+=coagulopathic; a=significantly different from healthy controls; b=significantly different from minor trauma; c=significantly different from TIC-; ISS=injury severity score.

Thromb Res. 2014 September ; 134(3): 652–658

New insights into acute coagulopathy in trauma patients

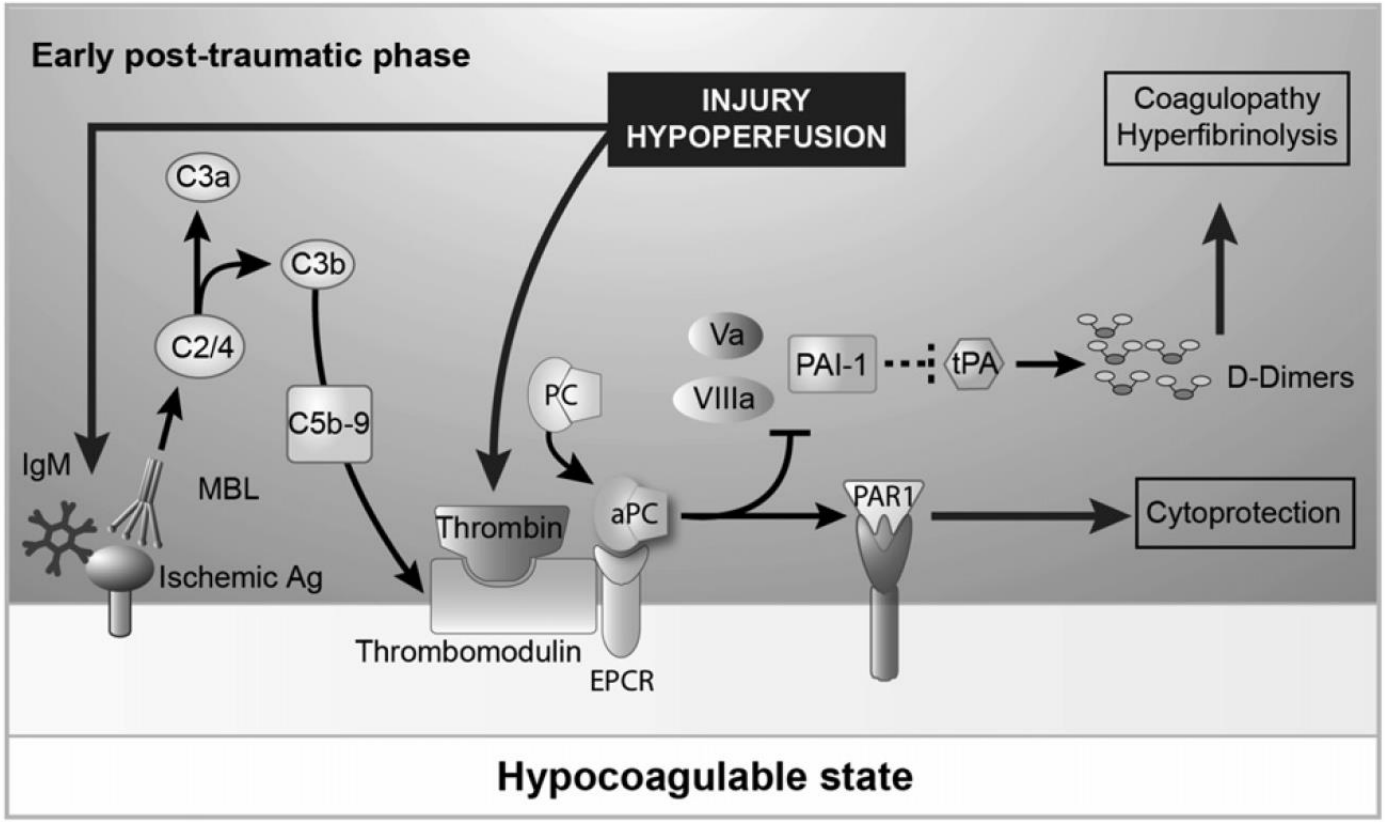

Fig. 1. Early post–traumatic phase. Tissue trauma and shock with systemic hypoperfusion appear to be the primary factors responsible for the development of acute traumatic coagulopathy in the immediate post–injury phase. As a result of overt activation of protein C pathway, the acute traumatic coagulopathy is characterised by *coagulopathy* (de–activation of the coagulation factors Va and VIIIa) in conjunction with *hyperfibrinolysis* (de–repression of fibrinolysis). In addition to its anticoagulant effects, activated protein C proteolytically activates the cell surface receptor, protease–activated receptor–1 (PAR–1), to produce several *cytoprotective* effects including anti–inflammatory properties, anti–apoptotic activity and protection of endothelial barrier function, all being required for acute survival during shock. The complement cascade is being activated immediately after trauma via the lectin pathway (mannose binding lectin, MBL), amplified via the alternative pathway and seems to be implicated in the activation of the protein C pathway early after severe trauma.

Best Practice & Research Clinical Anaesthesiology 24 (2010) 15–25

Cause of trauma-induced coagulopathy

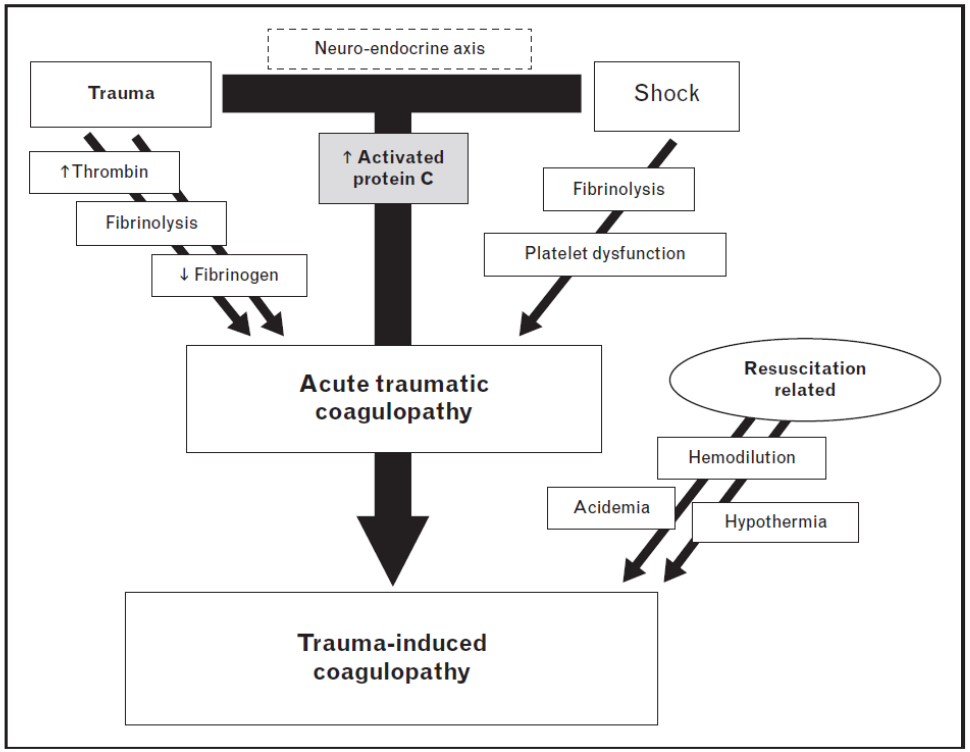

FIGURE 1. Pathogenesis of trauma-induced coagulopathy. Trauma-induced coagulopathy is the global failure of haemostasis after major trauma haemorrhage. Hemodynamic shock and tissue trauma immediately activate the neuro-endocrine axis and initiate an early endogenous process mediated by the protein C pathway – acute traumatic coagulopathy. Tissue injury leads to increased thrombin generation, fibrinolysis secondary to release of tissue plasminogen activator and early fibrinogen depletion (potentially via direct fibrinogenolysis). In the presence of severe shock, these changes result in systemic activation of protein C through the thrombin-thrombomodulin complex with resulting anticoagulation, massive fibrinolytic activity, platelet dysfunction, and further fibrinogen loss. Early changes in coagulation are exacerbated by iatrogenic factors or inadequate resuscitation, for example, unbalanced blood product replacement or crystalloid infusion producing haemodilution, hypothermia, and acidemia. Individual coagulation phenotype is dependent on severity of shock and degree of injury.

Curr Opin Anesthesiol 2016, 29:212–219

Comparative Response of Platelet fV and Plasma fV to Activated Protein C and Relevance to a Model of Acute Traumatic Coagulopathy

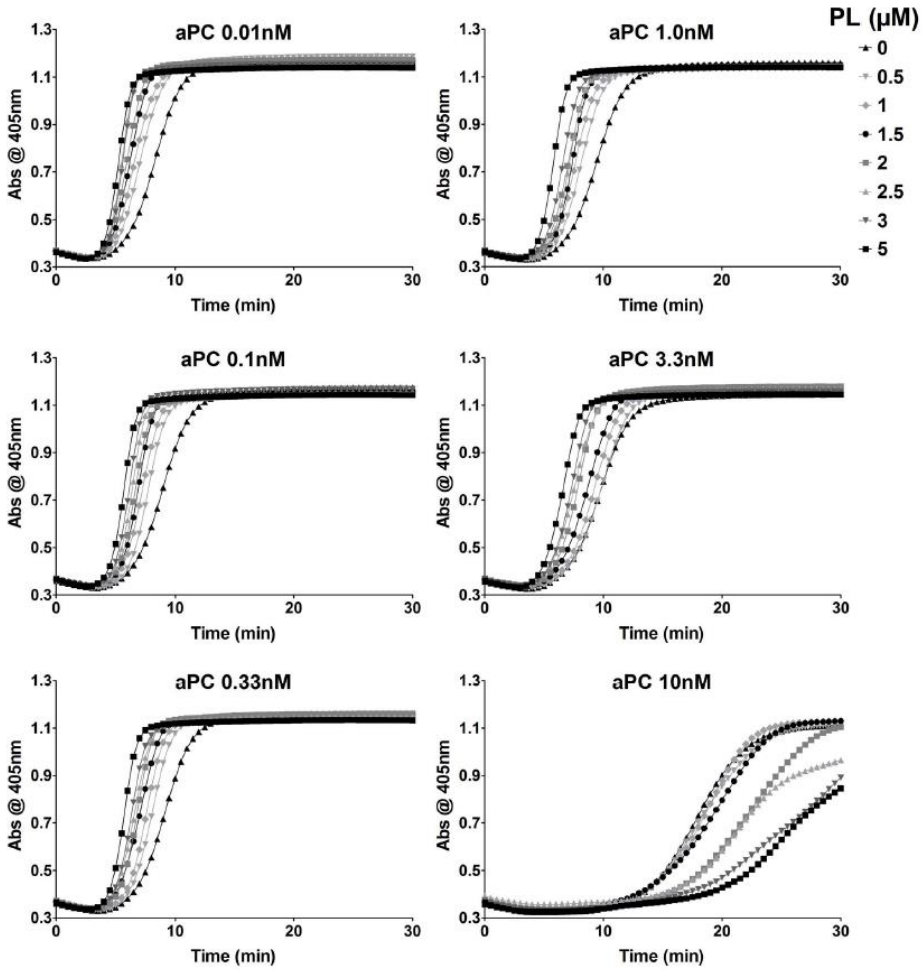

Figure 7. aPC concentrations below 10 nM have no significant effect on PL acceleration of clotting in PFP. In the turbidimetric assay, fibrin crosslinking corresponds to an increase in absorbance at 405 nm wavelength. Increasing the amount of available PL reduced the time for the initiation of fibrin crosslinking and increased the rate of fibrin crosslinking but had no effect on the maximum fibrin crosslinking as observed for all concentrations of aPC below 10 nM. aPC concentrations above 10 nM did not display any fibrin crosslinking within the first 30 min, and PL no longer provides any procoagulant benefit. Curves are averages of three independent plasma samples.
doi:10.1371/journal.pone.0099181.g007

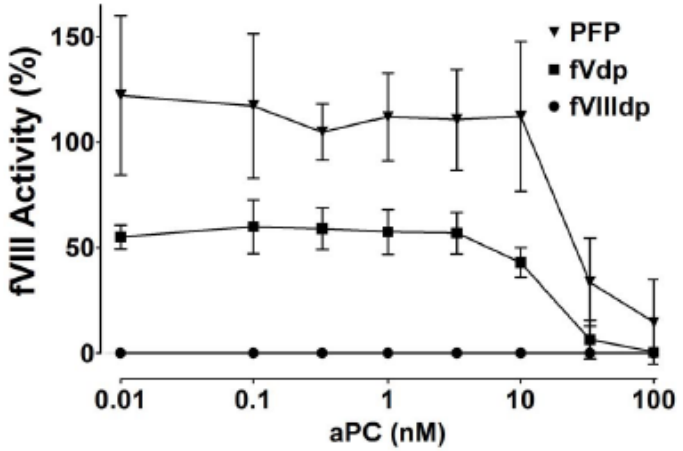

Figure 8. Nanomolar amounts of aPC are required to degrade fVIII activity. In fresh PFP, no change in fVIII activity by aPC was observed until a dose >10 nM ($p<0.001$). fVdp showed a similar trend ($p<0.05$ that 3.3 nM and 100 nM aPC are different); fVIIIdp was used as a negative control. The mean and standard deviation of four PFP samples is shown; fVdp and fVIIIdp are means and standard deviations of two technical replicates.
doi:10.1371/journal.pone.0099181.g008

Assistances Circulatoires

Mechanisms of Bleeding and Approach to Patients With Axial-Flow Left Ventricular Assist Devices

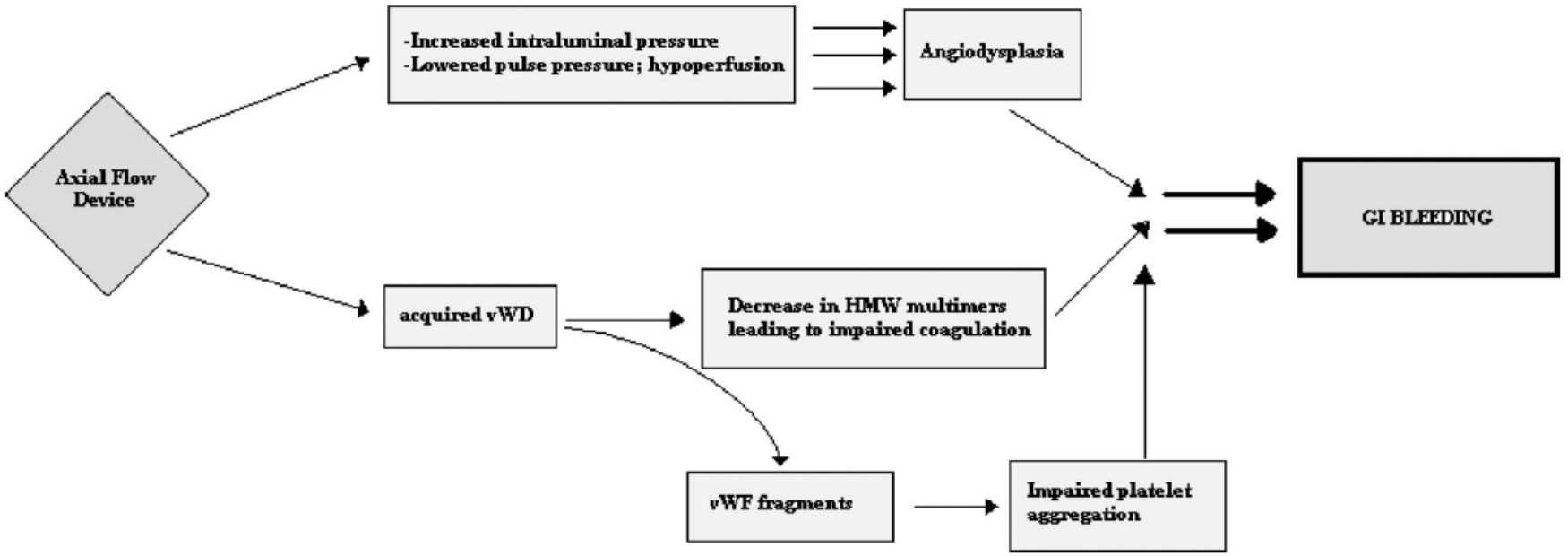

Figure 2. Mechanisms implicated in gastrointestinal (GI) tract bleeding in patients with axial-flow left ventricular assist devices (LVADs): Patients treated with axial-flow LVADS are at increased risk of developing GI tract bleeding. There are several mechanisms implicated with these increased risks. The device leads to increased intraluminal pressure and lowered pulse pressure, resulting in hypoperfusion of the intestines. These physiological changes result in an increased risk of developing angiodysplasia. These devices also decrease the high-molecular-weight (HMW) von Willebrand factor (vWF) multimer size because of excessive cleavage by the metalloprotease ADAMTS13. This results in an acquired form of vWF disease. Although not studied in detail, vWF fragments from the breakdown of HMW multimers could be involved in the inhibition of platelet aggregation. These mechanisms work synergistically to cause GI tract bleeding.

Circ Heart Fail **November 2011**

Circulatory support devices: fundamental aspects and clinical management of bleeding and thrombosis

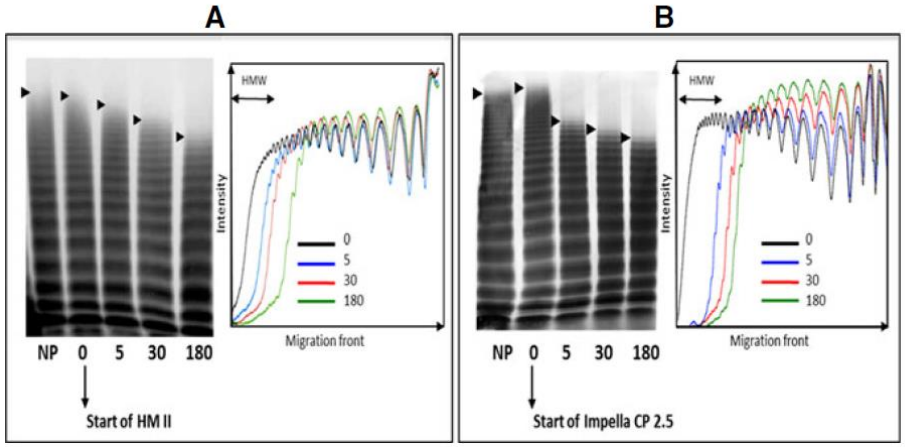

Fig. 1. Immediate loss of high molecular weight multimers (HMWMs) on high shear stress at the initiation of use of axial continuous-flow devices. (A, B) Representative time course of HMWM loss (with densitometric analysis) after the initiation of use of the HeartMate-II (HM-II) *in vitro* (A) or the Impella 2.5 (B). Black arrows indicate the front migration. NP, normal human pooled plasma.

Suzen et al, Journal of Thrombosis and Haemostasis, 13: 1757–1767

Acquired von Willebrand factor deficiency caused by LVAD is ADAMTS-13 and platelet dependent

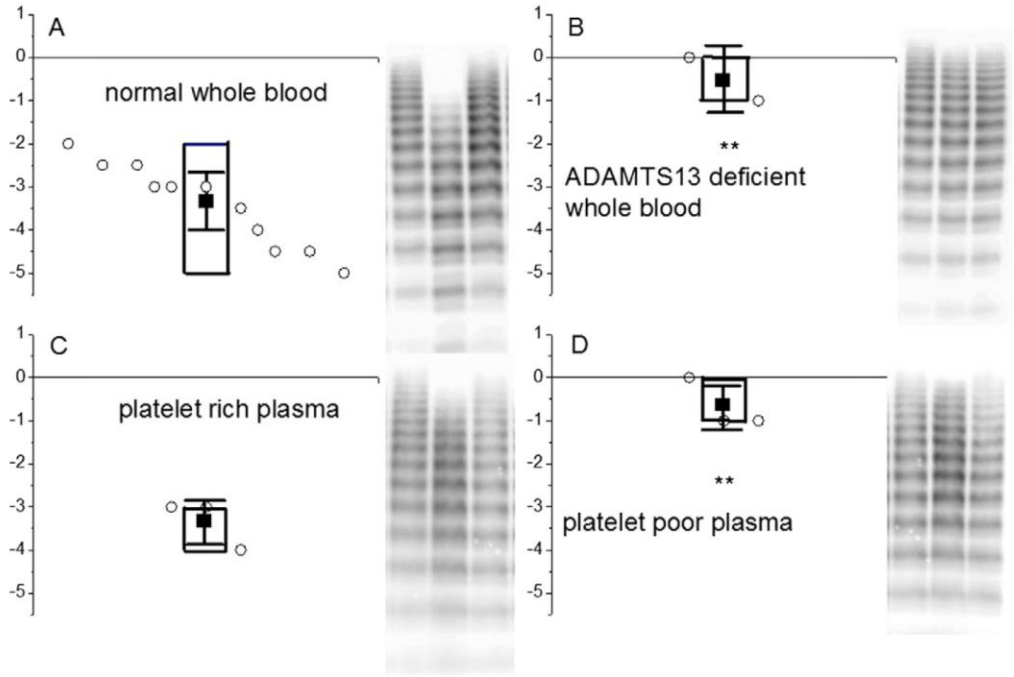

Fig. 2. Reduction inmultimer bands after 2 h of extracorporeal circulation in left ventricular assist device circuit. A) normalwhole blood; B)ADAMTS-13 deficient patients with thrombotic thrombocytopenic purpura, C) normal platelet rich plasma; D) normal platelet poor plasma. **p ≤ 0.005 A vs. B and A vs. D. Box plots show mean ± SD and ranges; individual values are depicted by open circles and ordered by magnitude of effect size. Multimer patterns depict representative experiments: lane 1 before, lane 2 after the extracorporeal circulation, lane 3 control plasma.

Table 1
Platelet aggregation in whole blood before and after extracorporeal circulation.

	Before extracorp. circulation	After extracorp. circulation
ADP (U)	77 (51–89)	19 (0–76)**
Arachidonic acid (U)	80 (23–100)	46 (0–102)**
Ristocetin (U)	116 (64–135)	51 (0–97)**
TRAP (U)	96 (77–107)	37 (0–73)**

Medians and the range; **$p < 0.005$; ($n = 12$).
ADP = adenosine diphosphate.
TRAP = thrombin receptor activating peptide.

Thrombosis Research 137 (2016) 196–201

Conclusion

- Physiopathologie complexe
- Influence des situations cliniques :

  trauma/obstétrique/assistances circulatoires
- Hypoxie cellulaire initiale: mortalité à court terme
- Inflammation/coagulopathie/ défaillance

  multiviscérale : mortalité retardée

Merci pour votre attention

LE PREMIER MODELE DE CHOC HEMORRAGIQUE

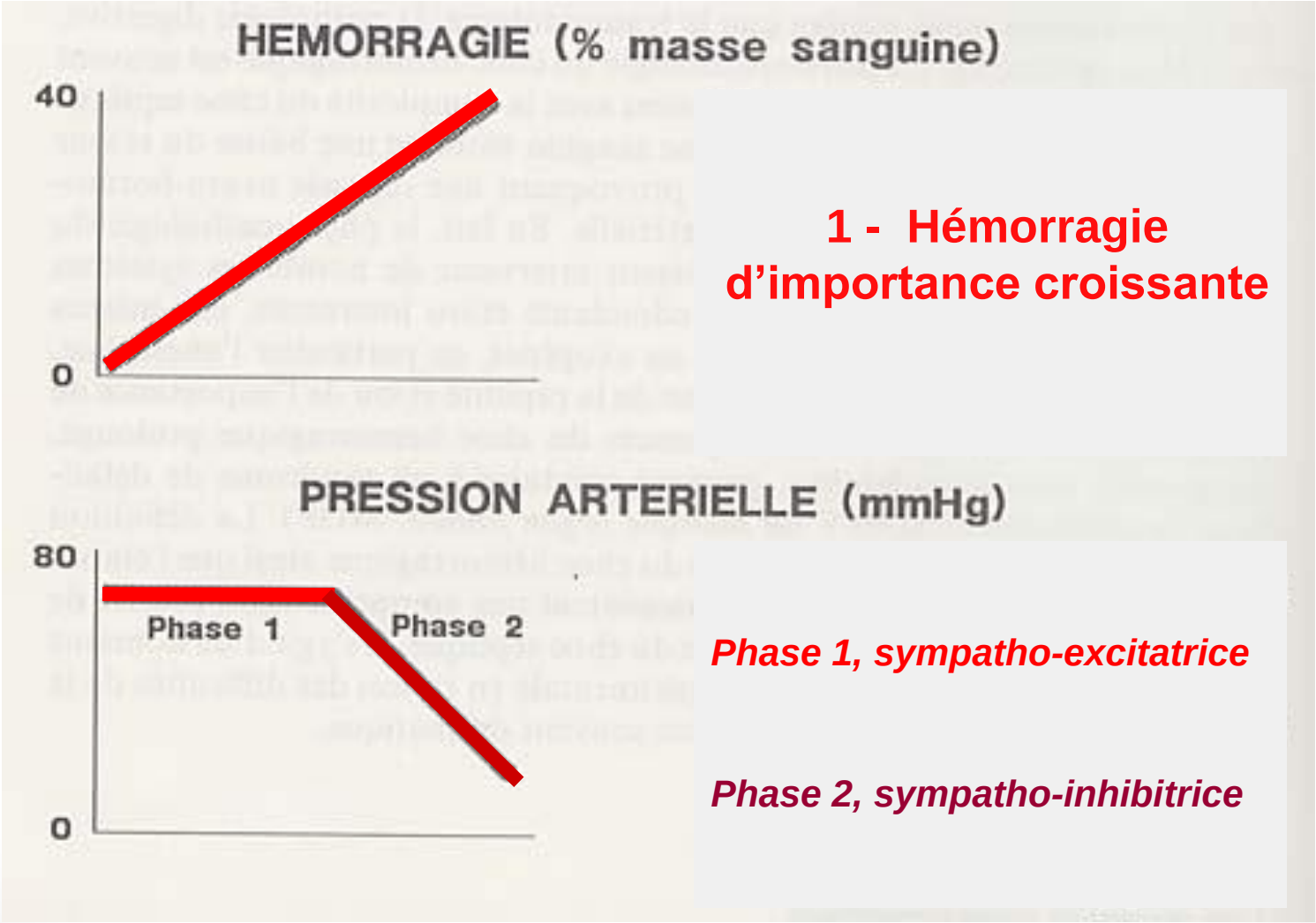

1 - Hémorragie d'importance croissante

Phase 1, sympatho-excitatrice

Phase 2, sympatho-inhibitrice

Early Platelet Dysfunction: An Unrecognized Role in the Acute Coagulopathy of Trauma

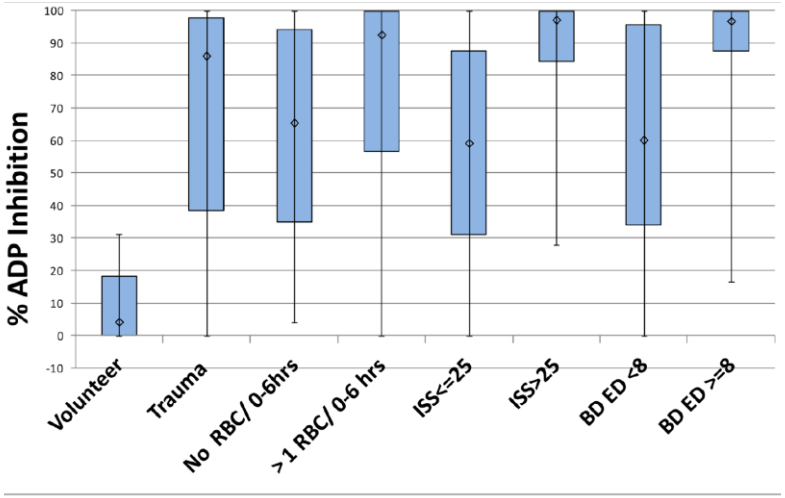

Figure 2.
Median % ADP Receptor Inhibition in trauma patients compared to healthy volunteers, including stratification according to shock (Base Deficit), blood transfusion (RBCs), and tissue injury (ISS).

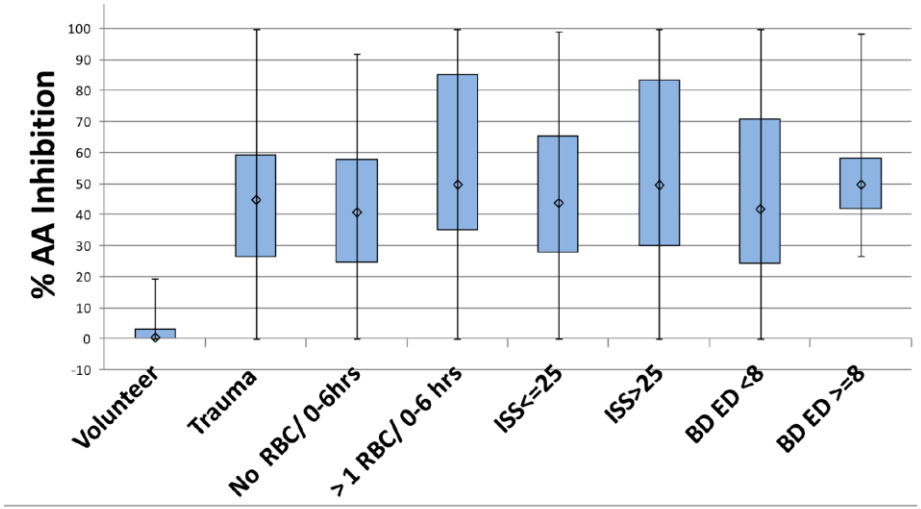

Figure 3.
Median % AA (TXA2) Receptor Inhibition in trauma patients compared to healthy volunteers, including stratification according to shock (Base Deficit), blood transfusion (RBCs), and tissue injury (ISS).

J Am Coll Surg. 2012 May ; 214(5): 739–746

LE DEUXIEME MODELE DE CHOC HEMORRAGIQUE

2 - Hémorragie pour obtenir un niveau de TA pré-déterminé, puis retransfusion

(**modèle de WIGGERS**)

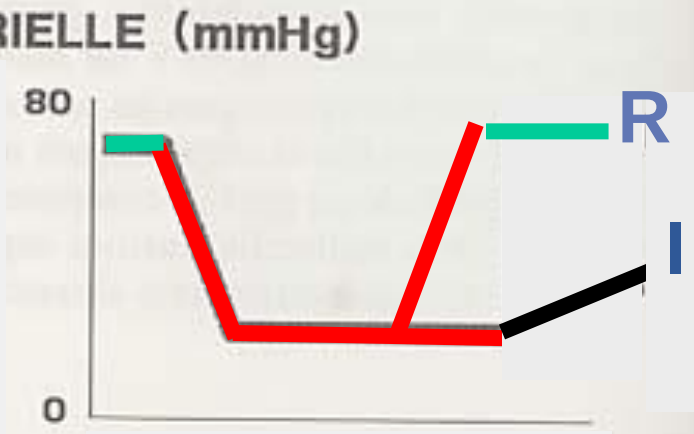

Normalisation après transfusion :
choc Réversible

Hypotension après transfusion :
choc Irréversible

Bradycardie paradoxale

- 7 % des chocs hémorragiques
- Hémorragie rapide et massive
- Réflexe vago-vagal
- Mécanorécepteurs intracardiaques

Barrriot et Riou, Intensive Care Med 1987

Hémorragie et Hypotension constante

Schlumberger et al, Br J Anaesth, 74, 42, 1995

% masse sanguine

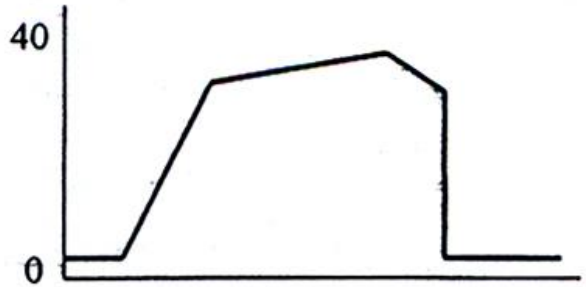

PA

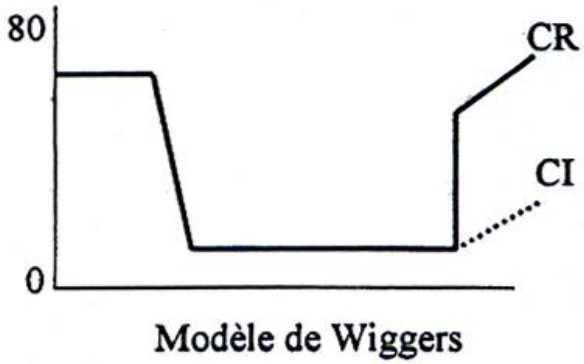

Modèle de Wiggers

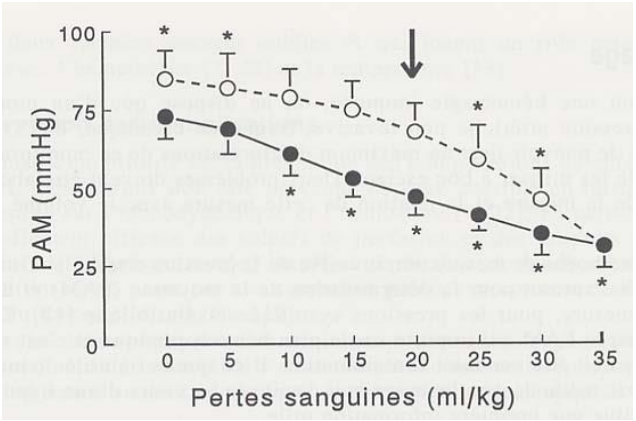

Transfusion immédiate

Transfusion retardée

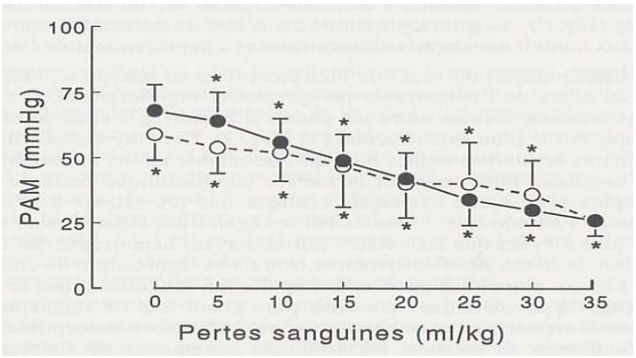

Physiopathologie du Choc Hémorragique

PM Mertes

Service d'Anesthésie Réanimation
Nouvel Hôpital Civil – CHU de Strasbourg
U 1116 /EA 3072 /FMTS
paul-michel.mertes@chru-strasbourg.fr

Amélioration du pronostic

- Techniques d'hémostase (chirurgie/embolisation)
- Traitement des coagulopathies
- Délivrance des PSL
- Technique de réchauffement
- Rapidité de correction du choc hémorragique
- Mortalité > 50 CG: 45 à 16 % de 1988 à 1993

Une physiopathologie complexe

- Choc Hypovolémique : hypoxie cellulaire et risque de mortalité … à court terme

- Réponse Adaptative (mal-adaptative?) :
  - Volume et rapidité de l'hémorragie, Mécanismes compensateurs, Durée du choc, Lésions associées
  - Composante Redistributive, Inflammation, Reperfusion, Défaillance Multiviscérale, Transfusion …

NEURAL MECHANISMS IN THE CARDIOVASCULAR RESPONSES TO ACUTE CENTRAL HYPOVOLAEMIA

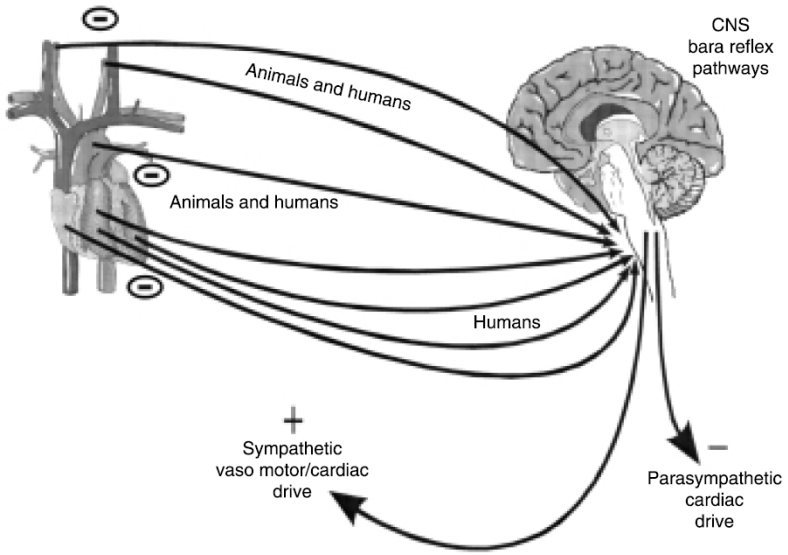

Fig. 2 Schematic diagram of the neural pathways mediating phase I of the response to acute central hypovolaemia. The circulatory adjustments that maintain arterial pressure during phase I of acute central hypovolaemia are dependent entirely on baroreflex-mediated increases in sympathetic drive and reductions in vagal drive. In dogs and rabbits, this response is exclusively due to unloading of arterial baroreceptors. In humans, there is some evidence that unloading of cardiac baroreceptors may also play some role, but this is indirect and far from conclusive. See text for further details.

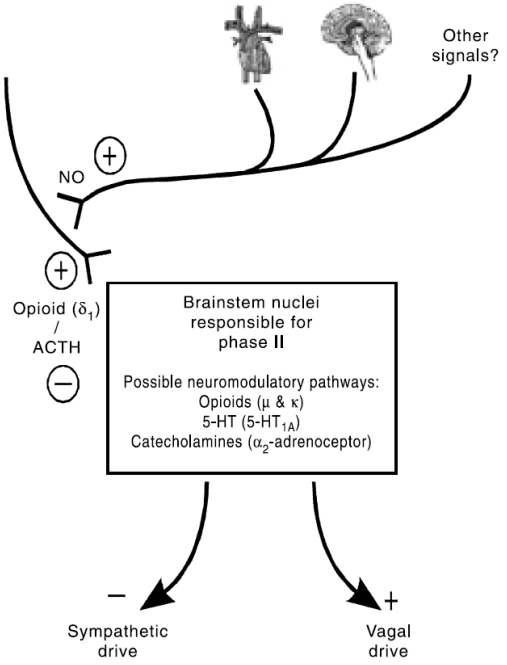

Fig. 3 Schematic diagram of the possible neural mechanisms mediating phase II of the response to acute central hypovolaemia. The precise nature of the stimuli initiating phase II remain unknown, but there is good evidence for contributions of (paradoxical) increased firing of cardiac (persumably left ventricular) afferents and signals from higher brain centres. There is good evidence that phase II depends on stimulation of both δ_1-opioidergic and nitrergic mechanisms in the brainstem. One possibility that is supported by experimental evidence (see text) is that activity in nitrergic neurons activates enkephalinergic neurons, which, in turn, leads to stimulation of δ_1-opioid receptors. Phase II is triggered by activation of brainstem δ_1-opioid receptors, but inhibited by adrenocorticotropic hormone (ACTH). Other neurotransmitter systems may also be involved in the brainstem pathways mediating phase II, including opioids acting at μ- and κ-opioid receptors, 5-hydroxytryptamine (5-HT) acting at 5-HT_{1A} receptors and catecholamines acting at α_2-adrenoceptors. The anatomical arrangement of these pathways remains unknown, but the nucleus tractus solitarius, rostral ventrolateral medulla and caudal mid-line medulla are candidate sites (see text for details). NO, nitric oxide.

Lubrock et al, Clinical and Experimental Pharmacology and Physiology (2001) **28**, 479–487

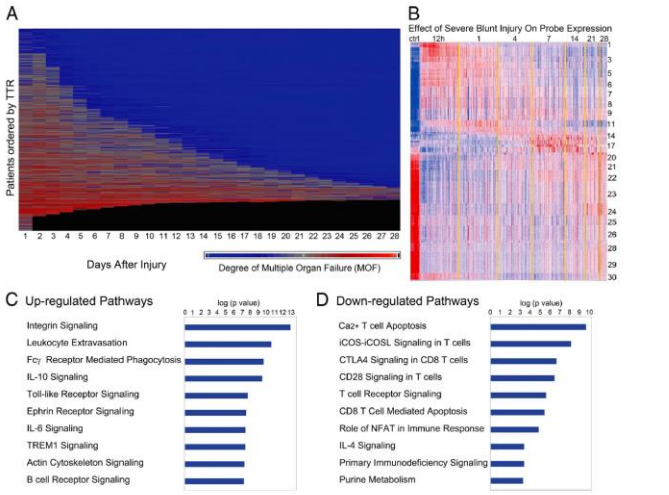

Figure 1. Organ injury and genomic changes associated with severe blunt trauma. (A) Whole blood was taken from severe blunt trauma patients, leukocytes were isolated, and total cellular RNA was extracted and hybridized onto an HU133 Plus 2.0 GeneChip. The continuum of clinical responses to severe blunt trauma in the 1,637 total patients from which the 167 sampling trauma patients were drawn is shown graphically. Each row represents an individual patient ordered by time to recovery (TTR), and the x axis represents time from injury in days. Patients are sorted from least to most severe organ injury and mortality. The presence and severity of organ injury is represented by colors from blue (least severe) to red (most severe). Black indicates death. (B) K-means clustering of the genes into 30 clusters based on patterns of expression over time. Red indicates increased and blue indicates decreased expression relative to the mean (white). 5,136 genes were differentially expressed between patients and controls (ctrl; FDR <0.001 and at least twofold change). (C and D) Summary of the canonical pathways most affected by trauma. The graph shows the −log10 (p value) of the enrichment of the pathway.

J. Exp. Med. Vol. 208 No. 13 2581-2590
www.jem.org/cgi/doi/10.1084/jem.20111354

A genomic storm in critically injured humans

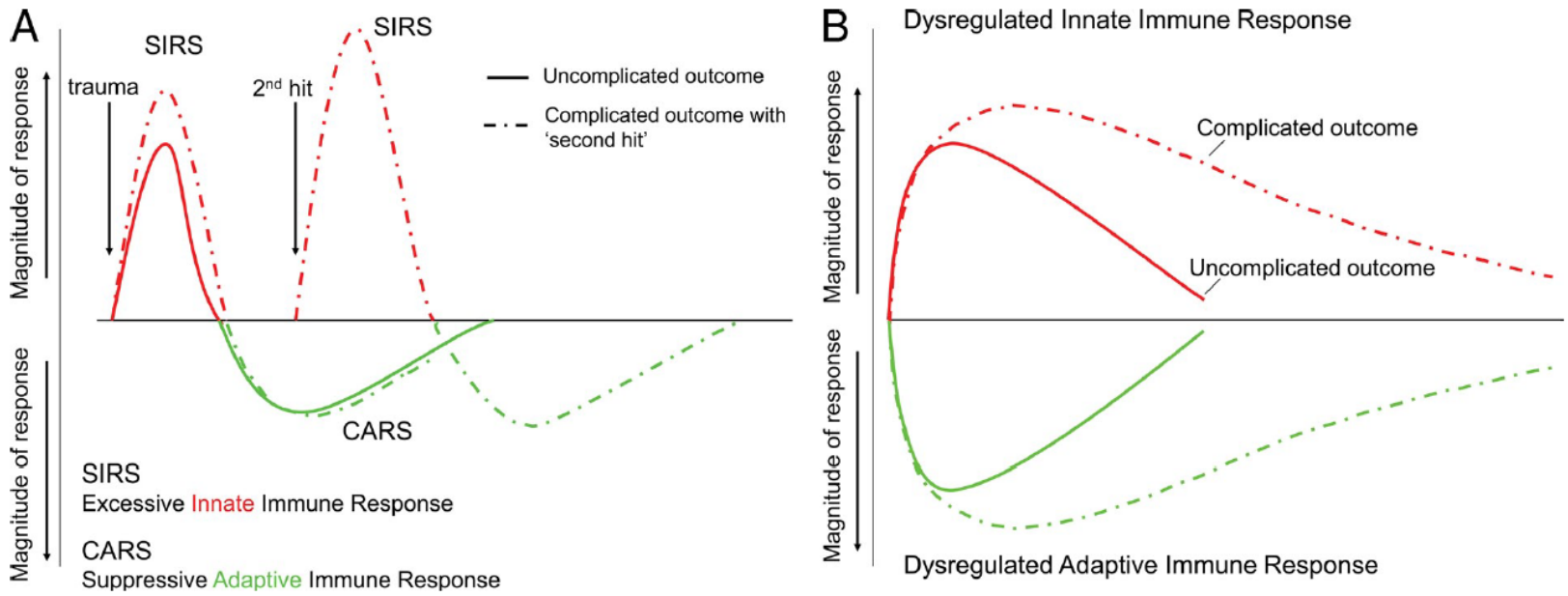

Figure 4. A genomic storm: Refining the immune, inflammatory paradigm in trauma. (A) The current paradigm explains complications of severe injury as a result of excessive proinflammatory responses (SIRS) followed temporally by compensatory antiinflammatory responses (CARS) and suppression of adaptive immunity. A second-hit phenomenon results from sequential insults, which leads to more severe, recurrent SIRS and organ dysfunction. (B) The proposed new paradigm involves simultaneous and rapid induction of innate (both pro- and antiinflammatory genes) and suppression of adaptive immunity genes. Complicated recoveries are delayed, resulting in a prolonged, dysregulated immune–inflammatory state.

J. Exp. Med. Vol. 208 No. 13 2581-2590
www.jem.org/cgi/doi/10.1084/jem.20111354

Cellular edema regulates tissue capillary perfusion after hemorrhage resuscitation

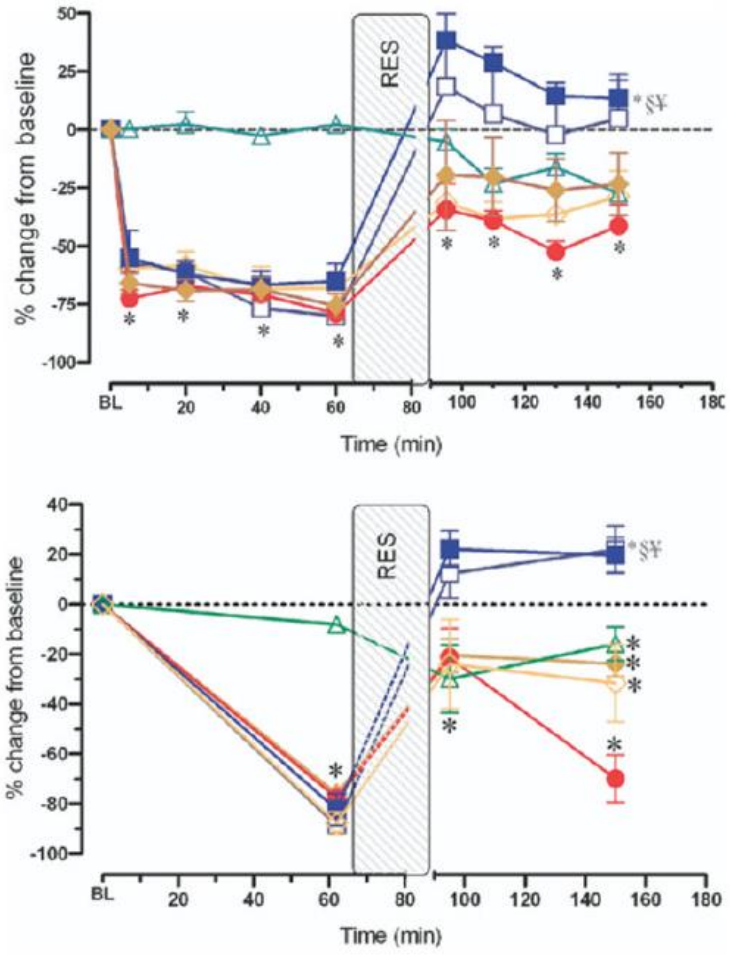

Fig 3.
Intestinal A1 blood flow (upper panel) and functional capillary density (lower panel), each expressed as a percentage change from corresponding baseline after hemorrhagic shock + conventional resuscitation (solid circles); hemorrhagic shock + conventional resuscitation + Amiloride simultaneously with resuscitation (open diamonds); hemorrhagic shock + conventional resuscitation + Amiloride preemptively at the beginning of hemorrhagic shock (solid diamonds); hemorrhagic shock + conventional resuscitation + DPR (solid squares); hemorrhagic shock + conventional resuscitation + DPR + Amiloride simultaneously with resuscitation (open squares); and after instrumentation, time-matched and Amiloride administration but no hemorrhage controls (open triangles). *$P < .01$ versus corresponding baseline by repeated-measures 1-way ANOVA followed by Dunnett's multiple-range test, §$P < .01$ for the simulated DPR group versus the conventional resuscitation group by 2-way ANOVA followed by Bonferroni multiple comparison post-tests, ¥$P < .05$ for the simulated DPR group versus the sham no hemorrhage group by 2-way ANOVA followed by Bonferroni multiple comparison post-tests.

Surgery. 2007 October ; 142(4): 487–496.e2.

The European guideline on management of major bleeding and coagulopathy following trauma: fourth edition

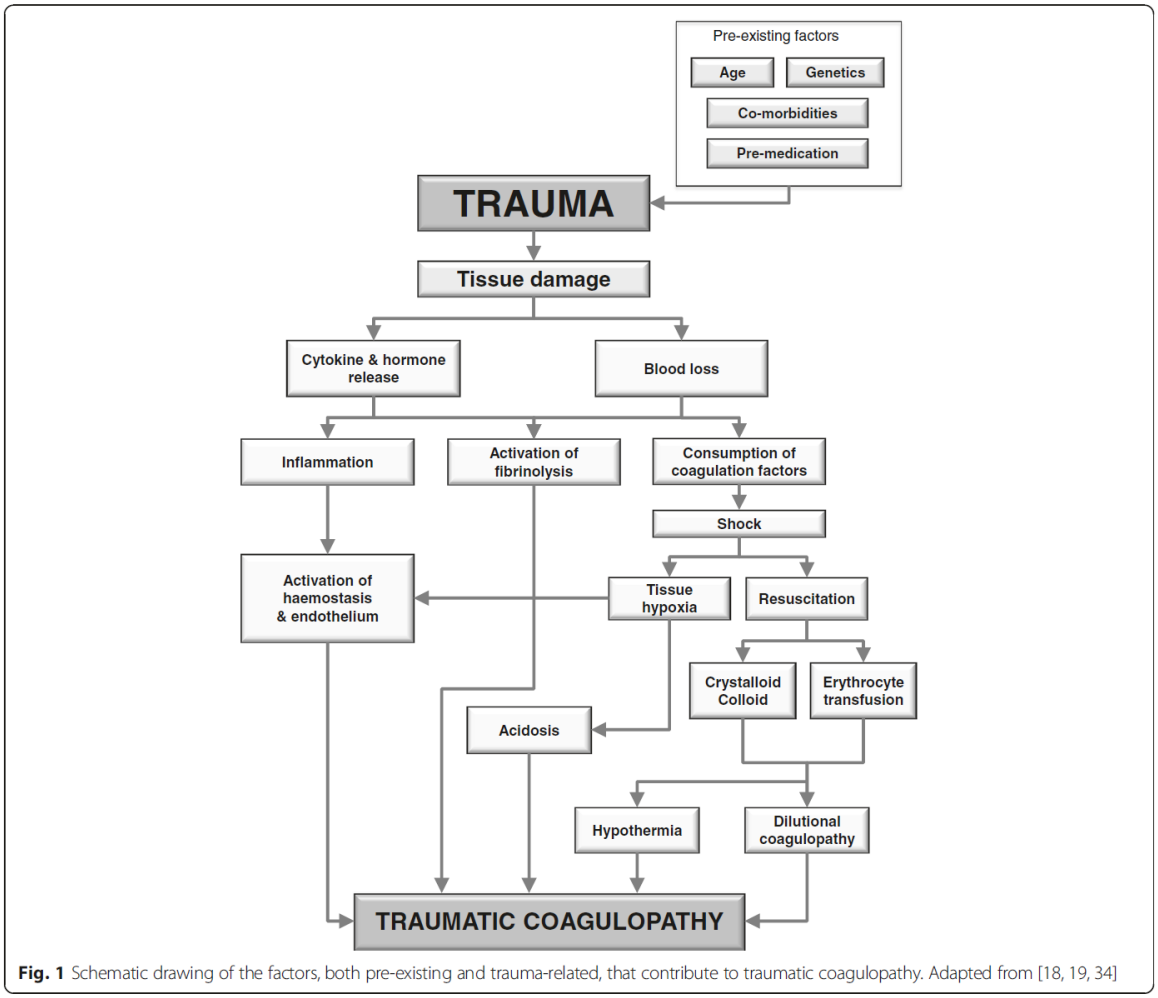

Fig. 1 Schematic drawing of the factors, both pre-existing and trauma-related, that contribute to traumatic coagulopathy. Adapted from [18, 19, 34]

Rossaint et al. Critical Care (2016) 20:100

Coagulopathy after severe pediatric trauma: A review

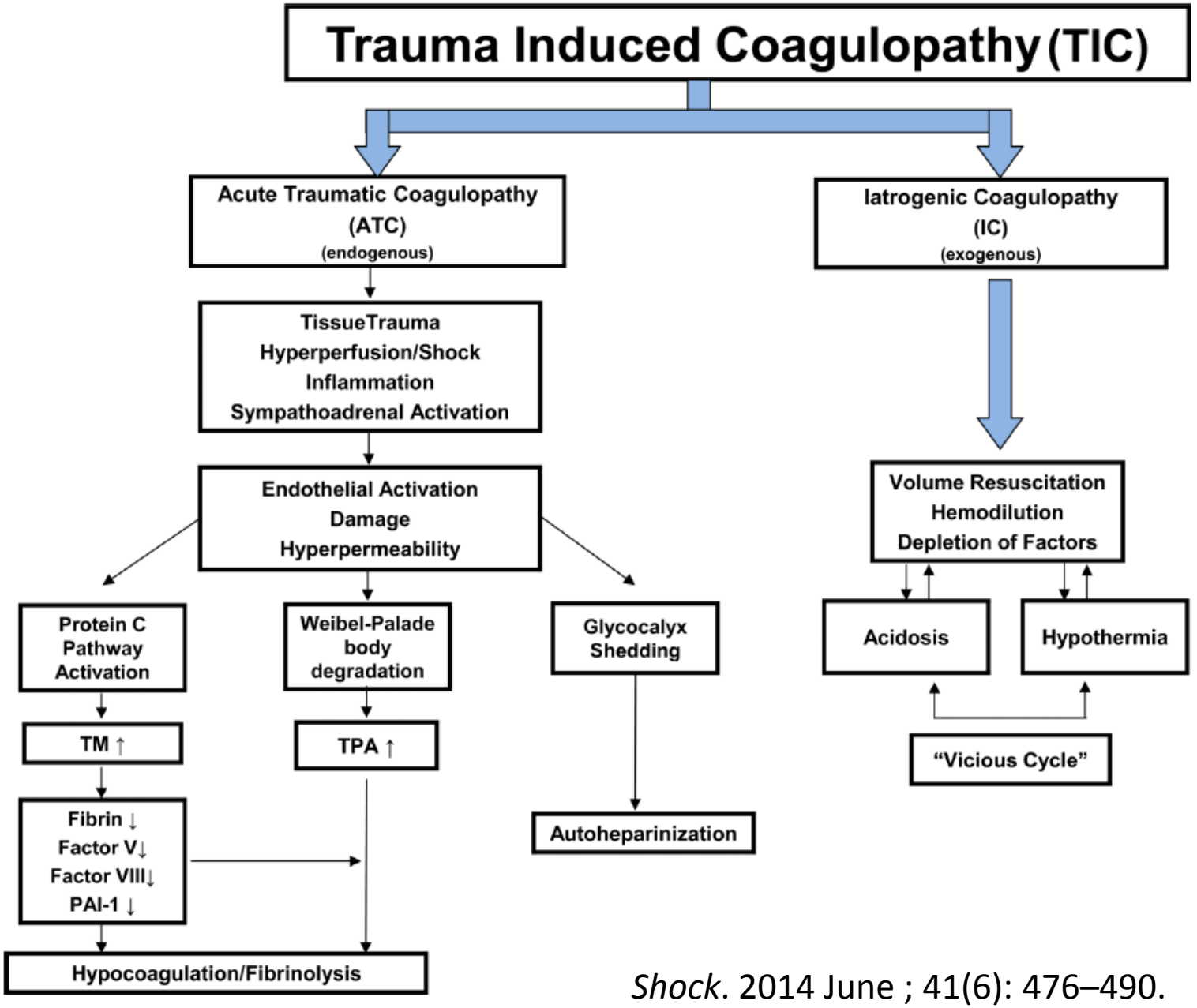

Shock. 2014 June ; 41(6): 476–490.

TLR2 ON BONE MARROW AND NON-BONE MARROW DERIVED CELLS REGULATES INFLAMMATION AND ORGAN INJURY IN COOPERATION WITH TLR4 DURING RESUSCITATED HEMORRHAGIC SHOCK

SHOCK, Vol. 46, No. 5, pp. 519–526, 2016

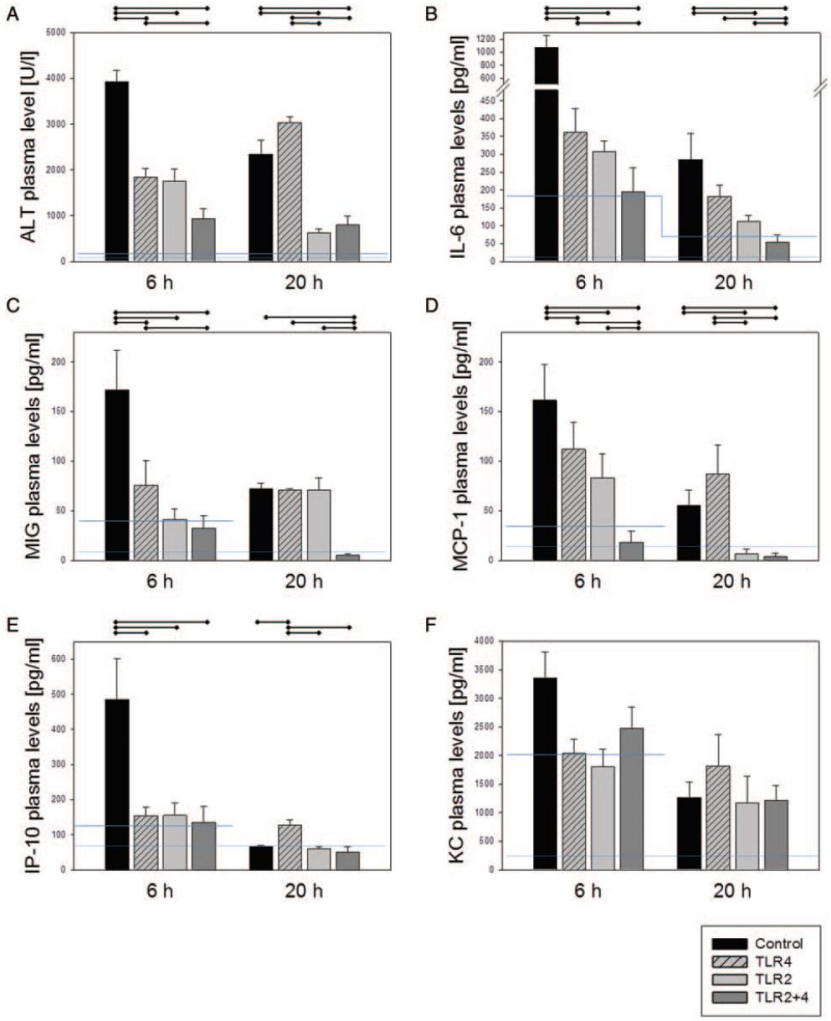

FIG. 5. **C57/Bl6 mice were pretreated with 100 μg of control mAB or T2.5 mAB and/or 5E3 mAB 30 min before H/R procedure.** A, ALT plasma levels in U/L are displayed. B–F, IL-6, MIG, MCP-1, IP-10, and KC are shown at two different time points (6 and 20 h). Significant differences between two groups are marked by a line on top of the bars. Blue lines illustrate mean plasma levels of sham control mice, dotted line illustrates uninjured control plasma levels. ($n = 6–14$ per experimental group, $^*P < 0.05$, Data represent mean ± SEM).

Syncope vago-vagale

Démonstration de l'existence de 2 phases du choc hémorragique chez l'homme

Barcroft et al., Lancet 1944

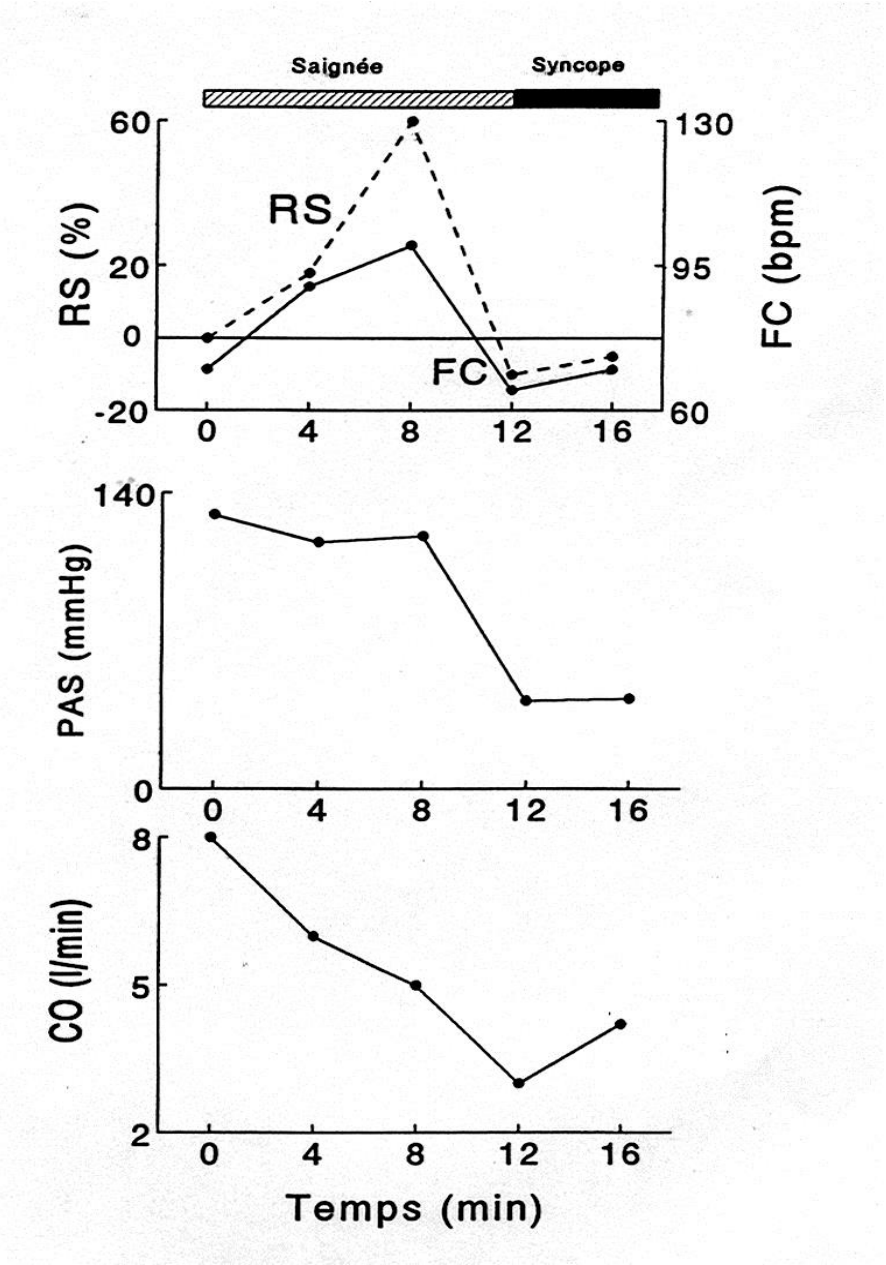

Prevalence, predictors and outcome of hypofibrinogenaemia in trauma: a multicentre observational study

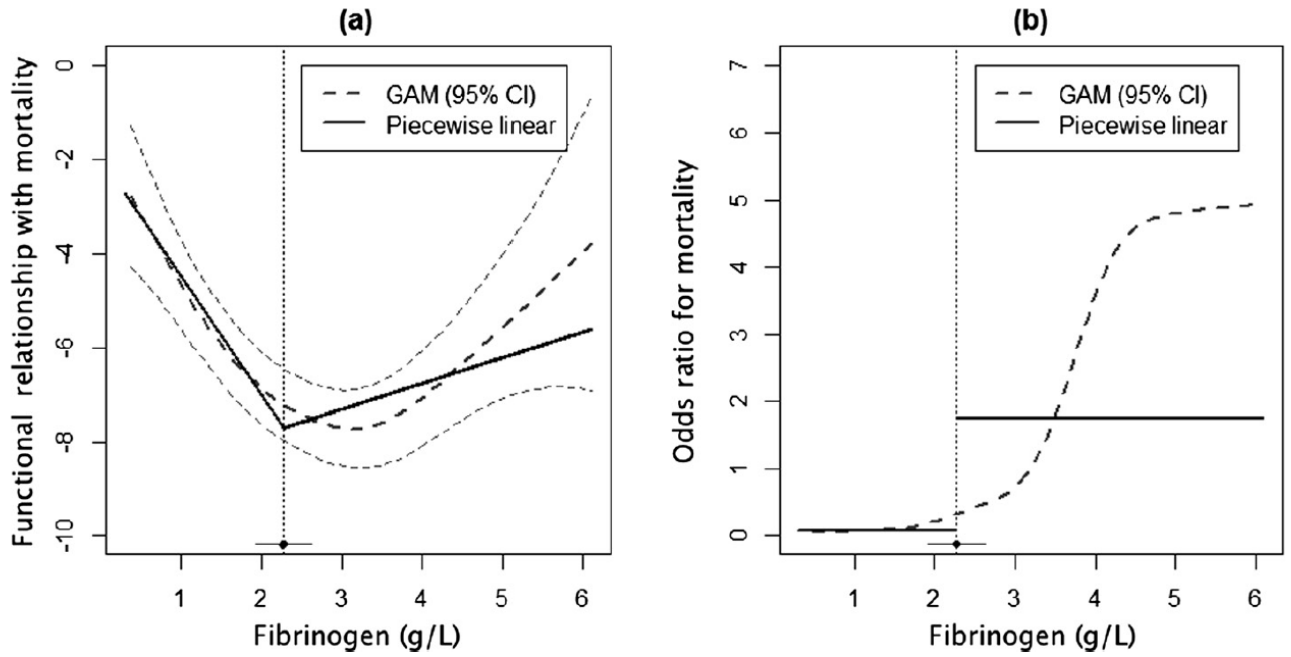

Figure 1 Multivariable generalised additive model and piecewise linear model for relationship between fibrinogen concentration and 28-day survival. Results from the multivariable generalised additive model (GAM) and the piecewise linear model for the relationship between fibrinogen concentration and 28-day survival, adjusted for Injury Severity Score, age, time from injury, mechanism of injury, base excess, International Normalized Ratio, platelet count and gender. The functional relationship is clearly nonlinear **(a)**, resulting in a corresponding nonconstant odds ratio across the observed range of fibrinogen values **(b)**. For the piecewise linear model, the breakpoint (95% confidence interval (CI)) is estimated at 2.29 (1.93, 2.64).

Hagemo et al. Critical Care 2014, 18:R52